UNIVERSITEIT • STELLENBOSCH • UNIVERSITY

A comparative analysis of the G1/S transition control in kinetic models of the eukaryotic cell cycle

by

Riaan Conradie

Thesis presented for the degree of Doctor of Philosophy in the Faculty of Science

Department of Biochemistry
University of Stellenbosch
Private Bag X1, 7602 Matieland, South Africa

Study leader: Prof J.L. Snoep

December 2009

Declaration

By submitting this dissertation electronically, I declare that the entirety of the work contained therein is my own, original work, that I am the owner of the copyright thereof (unless to the extent explicitly otherwise stated) and that I have not previously in its entirety or in part submitted it for obtaining any qualification.
Date: November 24, 2009

Abstract

A comparative analysis of the G1/S transition control in kinetic models of the eukaryotic cell cycle

R. Conradie

Department of Biochemistry
University of Stellenbosch
Private Bag X1, 7602 Matieland, South Africa

Thesis:

December 2009

The multiplication of cells proceeds through consecutive phases of growth and division (G1, S, G2 and M phases), in a process known as the cell cycle. The transition between these phases is regulated by so-called checkpoints, which are important to ensure proper functioning of the cell cycle. For instance, mutations leading to faulty regulation of the G1/S transition point are seen as one of the main causes of cancer.

Traditionally, models for biological systems that show rich dynamic behavior, such as the cell cycle, are studied using dynamical systems analysis. However, using this analysis method one cannot quantify the extent of control of an individual *process* in the system. To understand system properties at the *process* level, one needs to employ methods such as metabolic control analysis (MCA). MCA was, however, developed for steady-state systems, and is thus limited to the analysis of such systems, unless the necessary extensions would be made to the framework.

The central question of this thesis focuses on quantifying the control in mathematical models of the G1/S transition by the individual cell cycle processes. Since MCA was never applied to the cell cycle, several new methods needed to be added to the framework. The most important extension made it possible to follow and quantify, during a single cell cycle, the control properties of the individual system processes.

Subsequently, these newly developed methods were used to determine the control by the individual processes of an important checkpoint in mammalian cells, the restriction point. The positioning of the restriction point in the cell cycle was distributed over numerous system processes, but the following processes carried most of the control: reactions involved in the interplay between retinoblastoma protein (Rb) and E2F transcription factor, reactions responsible for the synthesis of Delayed Response Genes and Cyclin D/Cdk4 in response to growth signals, the E2F dependent Cyclin E/Cdk2 synthesis reaction, as well as the reactions involved in p27 formation. In addition it was shown that these reactions exhibited their control on the restriction point via the Cyclin E/Cdk2/p27 complex. Any perturbation of the system leading to a change in the restriction point could be explained via its effect on the Cyclin E/Cdk2/p27 complex, showing a causal relation between restriction point positioning and the concentration of the Cyclin E/Cdk2/p27 complex.

Finally, we applied the new methods, with a modular approach, to compare a number of cell cycle models for *Saccharomyces cerevisiae* (budding yeast) and mammalian cells with respect to the existence of a mass checkpoint. Such a checkpoint ensures that cells would have a critical mass at the G1/S transition point. Indeed, in budding yeast, a correction mechanism was observed in the G1 phase, which stabilizes the size of cells at the G1/S transition point, irrespective of changes in the specific growth rate. This in contrast to the mammalian cell cycle models in which no such mass checkpoint could be observed in the G1 phase.

In this thesis it is shown that by casting specific questions on the regulation and control of cell cycle transition points in the here extended framework of MCA, it is possible to derive consensus answers for subsets of mathematical models.

Uittreksel

A comparative analysis of the G1/S transition control in kinetic models of the eukaryotic cell cycle

R. Conradie

Departement Biochemie
Universiteit van Stellenbosch
Privaatsak X1, 7602 Matieland, Suid-Afrika

Tesis:

Desember 2009

Die selsiklus bestaan uit agtereenvolgende groei- en delingsiklusse wat tot selvermeerdering lei. Die siklus word gekenmerk deur onderskeie fases (G1, S, G2 en M) wat deur sogenaamde beheerpunte gereguleer word. Hierdie beheerpunte verseker dat selvermeerdering nie ongekontroleerd kan plaasvind nie en mutasies wat lei tot foutiewe regulering van die G1/S transisiepunt word as een van die hoofoorsake van kanker beskou.

Die hoofdoel van hierdie studie was om die beheer wat selsiklusprosesse op die G1/S transisie uitoefen met behulp van wiskundige modelle te kwantifiseer. Omdat biologiese sisteme soos die selsiklus ryk dinamiese gedrag vertoon, word hulle tradisioneeldeur middel van dinamiese sisteemanalise bestudeer. Die analisemetode beskik egter nie oor die vermoë om die hoeveelheid beheer wat afsonderlike sisteem*prosesse* op ′n sisteemeienskap uitoefen te kwantifiseer nie. Om sisteemeienskappe op *proses*vlak te verstaan moet metodes soos metaboliese kontrole analise (MKA) ingespan word. MKA was egter ontwikkel om sisteme in ′n bestendige toestand te analiseer en aangesien MKA nog

nooit vantevore vir selsiklus analises gebruik was nie, moes nuwe MKA tegnieke gedurende die studie ontwikkel word. Die belangrikste van die metodes maak dit moontlik om beheer (soos uitgeoefen deur die onderskeie sisteemprosesse) oor ′n enkele selsiklus na te volg en te kwantifiseer. Die nuut-ontwikkelde metodes was vervolgens gebruik om te bepaal hoe een so ′n beheerpunt in soogdierselle - die restriksiepunt - deur die onderskeie sisteemprosesse beheer word.

Die studie het aangedui dat die posisie van die restriksiepunt tydens die selsiklus deur ′n verskeidenheid sisteemprosesse beheer word. Die bevinding was dat vier prosesse beduidend meer beheer op die posisie van die restriksiepunt uitoefen: Reaksies wat betrekking het op die wisselwerking tussen retinoblastoma proteïen (Rb) en E2F transkripsiefaktor; reaksies verantwoordelik vir die sintese van vertraagde responsgene en Siklien D/Cdk4 in respons tot groeiseine; die E2F afhanklike Siklien E/Cdk2 sintesereaksie; sowel as die reaksies betrokke in p27 vorming. Daar was ook aangetoon dat hierdie reaksies hul beheer op die posisie van die restriksiepunt deur die Siklien E/Cdk2/p27 kompleks uitoefen, siende enige sisteemversteuringe (wat tot veranderinge in die restriksiepuntposisie aanleiding gee) deur veranderinge in die kompleks verklaar kon word - ′n observasie wat aandui dat daar ′n kousale verhouding is tussen die posisie van die restriksiepunt en die Siklien E/Cdk2/p27 kompleks.

Die nuut-ontwikkelde metodes was verder gebruik om ′n verskeidenheid selsiklusmodelle van *Saccharomyces cerevisiae* (bakkersgis) en soogdierselle met ′n modulêre aanpak te vergelyk om te bepaal of daar ′n massa beheerpunt in beide soogdier- en bakkersgisselle bestaan. Daar word gepostuleer dat hierdie beheerpunt verseker dat selle ′n kritiese massa by die G1/S transisiepunt bereik. Die resultate van die studie dui daarop dat bakkersgis, anders as soogdierselle, oor so ′n korreksiemeganisme beskik. Die meganisme stabiliseer die grootte van selle in die G1 fase ondanks veranderinge in die groeitempo van die selle, sodat massa homeostaties by die G1/S transisiepunt gehandhaaf word. Die studie het getoon dat moeilike vrae met betrekking tot die selsiklus beantwoord kan word deur van wiskundige modelle gebruik te maak en die probleme in die nuut-ontwikkelde metaboliese kontrole analise raamwerk te giet.

Dedications

Vir my pa en ma - die twee liefste mense wat ek ken.

Acknowledgements

- My supervisor and one of my best friends, Prof. Jacky L. Snoep, for his guidance, support, integrity (he always leads by example) and for exposing me to the field of Systems Biology in a much broader context than is set out in this thesis.

- The Triple-J group trio (Profs Jacky Snoep, Jannie Hofmeyr and Johann Rohwer) for creating a thought-provoking and stimulating research environment.

- Profs Hans V. Westerhoff and Bela Novak as well as Drs Frank Bruggeman, Attila Csikasz-Nagy and Andrea Ciliberto for their indespensible input to this research.

- Dr Franco du Preez, Packo Lamers, Christie Malherbe, Dr Brett Olivier, Christiaan Crous, Gerald Penkler, Du Toit Schabort and Francois du Toit for their friendship, support, and participation in many valuable discussions about my work.

- Mrs Lynette Eygelaar, Mrs Welma Maart and Mr Arrie Arends for invaluable administrative and technical support.

- Kora Holm for friendship, support and just for being *Kora*. Also, for proofreading and drawing of metabolic schemes found in Chapter 5.

- The National Bioinformatics Network (South Africa) for funding my research.

List of Publications

1. **Conradie R**, Westerhoff HV, Rohwer JM, Hofmeyr JH, and Snoep JL (2006) **Summation theorems for flux and concentration control coefficients of dynamic systems.** *Syst Biol (Stevenage)* **153**: 314-317.

2. Van Gend C, **Conradie R**, du Preez FB, Snoep JL (2007) **Data and model integration using JWS Online.** *In Silico Biology* **7(2 Suppl)**:S27-35.

3. Du Preez FB, **Conradie R**, Penkler GP, Holm K, van Dooren FLJ, Snoep JL (2008) **A comparative analysis of kinetic models of erythrocyte glycolysis.** *Journal of Theoretical Biology* **252(3)**: 488-496.

4. Snoep JL, van Gend C, **Conradie R**, du Preez FB, Penkler G, and Stoof C (2008) **JWS Online; a web-accessible model database, simulator and research tool.** In: *Experimental Standard Conditions of Enzyme Characterizations.* eds. Hicks, M.G. and Kettner, C. Logos Verlag, Berlin, Germany. pp 149-162.

5. Westerhoff HV, Kolodkin A, **Conradie R**, Wilkinson SJ, Bruggeman FJ, Krab K, van Schuppen JH, Hardin H, Bakker BM, Moné MJ, Rybakova KN, Eijken M, van Leeuwen HJ, Snoep JL (2009) **Systems biology towards life in silico: mathematics of the control of living cells.** *J Math Bio* **58(1-2)**:7-34.

6. **Conradie R**, Bruggeman, FJ, Ciliberto A, Csikasz-Nagy A, Novak B, Westerhoff HV, Snoep JL (2009) **Restriction point control of the mammalian cell cycle via the Cyclin E/Cdk2/P27 complex.** *Accepted for publication in FEBS Journal.*

Contents

List of Figures

List of Tables

Abbreviations

APC	Anaphase Promoting Complex
ATP	Adenosine Triphosphate
AU	Arbitrary Units
CA	Cyclin A/Cdk2 bound to CKI
CD	Cyclin D/Cdk4 bound to CKI
Cdc20A	Activator of APC in its active form
Cdc20I	Activator of APC in its inactive form
Cdh1, Cdh1A	Activator of APC (together with Cdc20)
Cdk1	Cyclin-dependent kinase that binds Cyclin B
Cdk2	Cyclin-dependent kinase that binds Cyclin A and Cyclin E
Cdk4	Cyclin-dependent kinase that binds Cyclin D
CE	Cyclin E/Cdk2 bound to CKI
CHX	Cycloheximide
CKI	Cyclin-Dependent Kinase Inhibitor
CLB2	B-type cyclin that occurs in S/G2/M phase and involved in mitosis
CLB5	B-type cyclins appearing during the late G1 phase
CLN2	Cyclin involved in budding process
CLN3	G1-cyclin involved in yeast START
CLN3p	Phosphorylated G1-cyclin involved in yeast START
DRG	Delayed Response Genes
ERG	Early Response Genes
E2F, SBF	Transcription factor for Cln2
G1 phase	First gap phase in cell cycle
G2 phase	Second gap phase in cell cycle

IEP	Intermediary Enzyme. Hypothetical protein activating Cdc20
M phase	Cell cycle phase comprising mitosis
MAP Kinase	Mitogen-Activated Protein Kinase
MCA	Metabolic Control Analysis
ODE	Ordinary Differential Equation
P27	Mammalian cyclin-dependent kinase inhibitor
PFK	Phosphofructokinase
PP-Rb	Hypophosphorylated Retinoblastoma
Ps	Critical cell mass
Rb	Retinoblastoma
SIC1	Cyclin-dependent Kinase inhibitor of Clb2 and Clb5

Chapter 1

General Introduction

The bewildering diversity of biological systems has been a near-endless source (and excuse) for biologists to isolate, identify and characterize components; leading to descriptions of biological systems as lists of parts. These descriptions have largely been qualitative; examples are lists of species in an ecosystem, or a list of the molecular components in a cell. Such a list can be seen as a blueprint for a system, which in itself is dead and not overly interesting, but forms a necessary start to study interactions between the species. The rich and functional behavior for which biological systems are known, stems from the interactions between its components and forms the key question for the field known as Systems Biology: "How can systems behavior be understood as a function of its components and their interactions?"

It is not essential to know all the components of a system to start analyzing the interactions between them, and often a semi-quantitative understanding of system behavior can be obtained by studying so called "core" - models, which include a minimal subset of components and interactions of the system, still leading to its characteristic behavior. Indeed, given the large number of components and the non-linearity of their interactions, it is often necessary to focus first on a subset of components and interactions. Even for such a subset of reactions to be analyzed, good mathematical tools are necessary and although some core models can be analyzed analytically, the vast majority of systems are analyzed

numerically using kinetic computer models.

With the rapid developments in the different *omics* fields, large data sets have become available, especially for the molecular parts of biological cells. In principle these datasets are again lists of components, but now a new level of detail is reached where the systems are completely described. The availability of experimental datasets at this level of detail and the necessity to make sense of all this information on a systems level have inspired new modeling approaches. As such we distinguish two modeling approaches: in so called "bottom-up" approaches, experimental data at the level of the components is used for model construction. These models can be very detailed and tend to integrate our current knowledge of the system, not so much attempt to fit the model on systems behavior. This in contrast to "top-down" approaches where systems behavior is used to construct the model[10].

Mathematical models have traditionally been applied to a number of biological disciplines such as ecology, neurology and metabolism. However, in most biological fields, for instance the whole field of molecular biology and cell biology, there is still a strong focus on molecular characterization. Although, in general, this also holds for the study of the cell cycle, where an enormous number of protein complexes are known to be involved, a number of research groups have actively been building and using mathematical models, ranging from core to detailed models, to describe the cell cycle.

Kinetic models are important tools for studying biological systems, not only to get a quantitative description of the system and for data analysis, but also to test hypotheses and to gain understanding. Specifically for the more detailed models, it is important to use good analysis tools for the interpretation of the model simulations. Traditionally, for systems displaying rich temporal behavior such as oscillations, bistability and chaos, a framework, loosely defined as dynamical systems analysis is used. Typical analyses performed in this framework include phase-plane, stability and bifurcation analysis, which are well suited for smaller systems but are not ideal for large systems (e.g. more than fifty reactions). Many biological systems have simpler dynamic behavior and, when kept in a constant environment, will reach a so-called steady state. Specifically

for the quantitative analysis of such systems a mathematical framework called metabolic control analysis (MCA) has been developed[48,38,40]. As its name suggest the framework has been often applied (but is not limited) to metabolic systems and has addressed important issues such as rate-limiting steps, and differences between regulation and control. Importantly for Systems Biology studies, the framework makes it possible to relate systemic properties to the characteristics of its components.

At the beginning of my PhD study, MCA had never been used in cell cycle studies, nor in the analysis of kinetic models of the cell cycle. Largely this could be attributed to the dynamic behavior that such systems display, very different from the steady states for which MCA was developed. A marked difference between the dynamical systems analysis and MCA is that in the first approach the analysis is often made in terms of variables (for instance in phase-plane analysis), while in the latter approach the analysis is cast in terms of processes, e.g. what is the control of an enzyme on the steady state flux? MCA has played an important role for the quantitative understanding of steady state systems, and it would be very interesting to see if the framework could be extended to dynamic systems such as the cell cycle, and to test whether such a different approach would help in understanding this complex and important biological phenomenon.

Cells reproduce by successive cycles of coordinated growth and division, resulting in a daughter and mother cell. For bacterial cells and fission yeast, the mother and daughter cells are identical, but for the budding yeast *Saccharomyces cerevisiae* the daughter cell is smaller than the mother cell, and the mother cell carries a scar for each bud she has produced. This process, called the cell division cycle, or cell cycle is shown schematically in Figure 1.1.

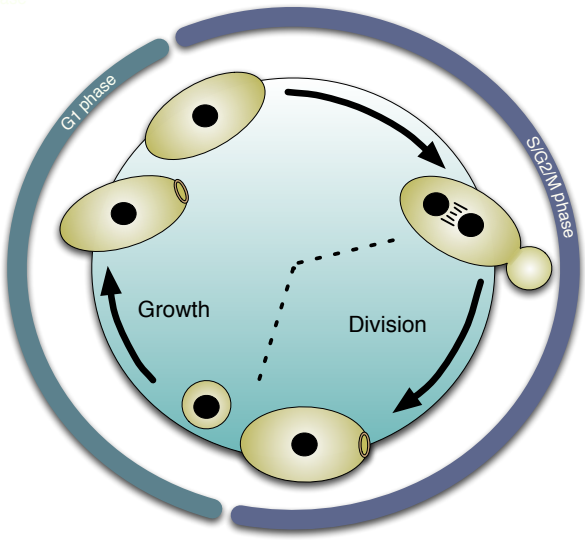

Figure 1.1: Coordinated growth and division cycles in *Saccharomyces cerevisiae*. Growth during the consecutive G1, S and G2 phases followed by the M phase (mitosis) and division are indicated for the budding yeast cell.

The cell cycle has been subdivided into the G1, S, G2 and M phases, progression between which is governed by checkpoints. The transition from the G1 phase to the S phase of the cell cycle is, in yeast, believed to be regulated by a mass checkpoint and in mammalian species an additional checkpoint exists in the form of the restriction point where cells assess the external conditions. Mutations leading to a deregulation of the G1 to S transition have been shown to be one of the main causes of cancer[84,58], clearly illustrating the importance of its control, the main subject of this thesis. Traditionally, cell biology and molecular biology studies focus on key players in the cell division cycle, such as the cyclins and cyclin dependent kinases and have shown that deregulation of these key players leads to phenotypic aberrations of the wild type cell cycle.

In this thesis: "A comparative analysis of the G1/S transition control in kinetic models of the eukaryotic cell cycle" I address the following question: Is it

possible to quantify the control exerted by the processes in the cell cycle network on the checkpoints of G1/S transition?

To address this question we had to develop several new methods, which were all based on the MCA framework. In Chapter 3 we extended this framework such that it could be applied to any dynamical system, and illustrated the approach for limit cycle oscillations and for a transient response in simple core models. Subsequently, using this method we analyzed the control distribution for the positioning of the restriction point in the mammalian cell cycle in Chapter 4. In addition, we reconciled the "species" and "processes" approaches, by analyzing in detail the correlation between the control by the processes on both the restriction point and the molecular species. In Chapter 5 we made a comparative analysis using a modular approach for the control on the G1/S transition and show that control on the G1/S transition is distributed over several processes to ensure that the critical cell mass at the G1 to S phase transition is not greatly compromised upon system perturbations.

We start with some background information on important topics that we treat in detail in this thesis.

Chapter 2

Background information on research topics

In this chapter I provide background information on the major research topics and methods that I use in my thesis. This includes an introduction in systems biology, modeling of the cell cycle and a short overview of metabolic control analysis. Each of the subsequent chapters has an introduction of its own, but these are rather short and immediately lead into the subject without extensive background.

Systems biologists try to get a quantitative understanding of the functional behavior of a biological system on the basis of the characteristics of its underlying components. A key methodology for the research field is the continuous iterative cycling between experiment and mathematical modeling. In addition to model validation, such cycles can also be used for the testing of hypotheses generated from the model. Subsequent model analysis in a suitable mathematical framework, such as Metabolic Control Analysis (MCA) can lead to a deeper understanding of emergent* system properties[68,67,82,78]. MCA is a rigorous framework[48,38,40] that quantifies the control of reaction steps on system properties. Originally MCA was developed to analyze steady state† behavior

*arising from the interactions of the components within a system.

†The stationary state in which the variables in a system remain constant in time but the

(see Section 2.3) but later extensions have been made to also include dynamical systems (Section 2.4).

Two different approaches have been used to construct mathematical models of biological systems: firstly the "bottom-up" approach, which relies on detailed information of the individual components and their interactions to examine the mechanism through which a system property emerges[10]. The second approach, called the top-down approach is more phenomenological [‡], and relies strongly on system information for its construction[10], whereas the "bottom-up" approach uses such information only for model validation. Both of these approaches and hybrids thereof have led to the construction of a multitude of detailed and core models for biological systems.

In a previous contribution[24] we have shown that MCA can be used to compare the functional behavior of steady state models of erythrocyte metabolism. In contrast to mathematical models of erythrocyte metabolism, mathematical models of the cell cycle (see Section 2.2) are dynamic, non steady state models that are constructed using a mixture of top-down and bottom-up approaches. After first introducing the biology of the cell cycle (Section 2.1), we will discuss these models in further detail (Section 2.2).

2.1 Cell cycle control

The process by which cells duplicate their contents and divide into two daughter cells is called the cell cycle or *cell-division cycle*. In eukaryotes the cell cycle is divided into two visually distinct periods called interphase and mitosis. During interphase the cell duplicates all its cellular components before undergoing mitosis during which the cell segregates its duplicated chromosomes and divides.

Three separate phases are distinguished in the interphase: G1, S and G2. The first gap phase (G1), in which proteins and RNA are synthesized, starts

reaction rates are non-zero

[‡]phenomenological models are not based on reaction mechanisms and, in most cases, they do not include knowledge about the interactions that occur between the molecular components[10]

directly after cell division and ends when DNA replication starts. This marks the beginning of the S phase which runs until all DNA has been replicated, leading to the second gap phase (G2), which lasts until the start of mitosis[75,76,51,15,14].

Traditionally, progression through the cell division cycle is believed to depend on discrete checkpoints, where a *decision* is made about transition to the next phase. Two such points are defined close to the G1/S transition: a mass assessing point and a restriction point. Both of these points are often referred to as the G1/S checkpoint, and this has led to the misconception that both points regulate the G1/S transition point in the same way. The mass assessing point is usually referred to as **START** in yeast. At this checkpoint a size requirement must be met before cells can transgress to the S phase, whereby balanced growth and division is ensured. When the functioning of this checkpoint is compromised by mutation, cells can become abnormally large or small[76,55]. In mammalian cells it is unclear whether such a strict mass assessment point exists. In these cells a **restriction point** is defined, which is a checkpoint where the cell senses external growth queues on basis of which a decision is made whether to transgress from the G1 phase to the S phase, or to enter the quiescent G0 phase. On the basis of the condition that is checked, we will make a strict distinction between the two G1/S checkpoints; to which we will refer as either **mass assessing point** or **restriction point**. Note that we will also make a distinction between checkpoints, where a check on a condition is made, and transition points which marks the actual transition from one phase to the next.

Along with the identification of the respective cell cycle phases and their checkpoints, a reductionistic or *protein-centric* approach has been followed by molecular and cell biologists to identify which proteins, regulate the respective cell cycle checkpoints. The most important kinases and phosphatases involved in the cell cycle regulation are the cyclins and cyclin dependent kinases (Cdks). The interaction between the cyclins and the anaphase-promoting complex (APC), which consists of a group of polypeptides and two auxilliary proteins (Cdc20 and Cdh1), is necessary to sustain a cell division cycle.

At the core of the cell cycle is a bistable loop emerging from the antagonism between the cyclin/Cdks and APC. During the G1 phase the Cdh1/APC concen-

tration is high and the cyclin/Cdk concentrations are low. The G1 to S phase transition is marked by a rapid increase in cyclin/Cdk concentrations and a decrease in the Cdh1/APC concentration (Figure 2.1). Additional bistable loops exist within the cell cycle to act as further points of regulation. An example is the antagonism between the retinoblastoma (Rb) protein and the E2F transcription factor essential for the establishment of the restriction point[84].

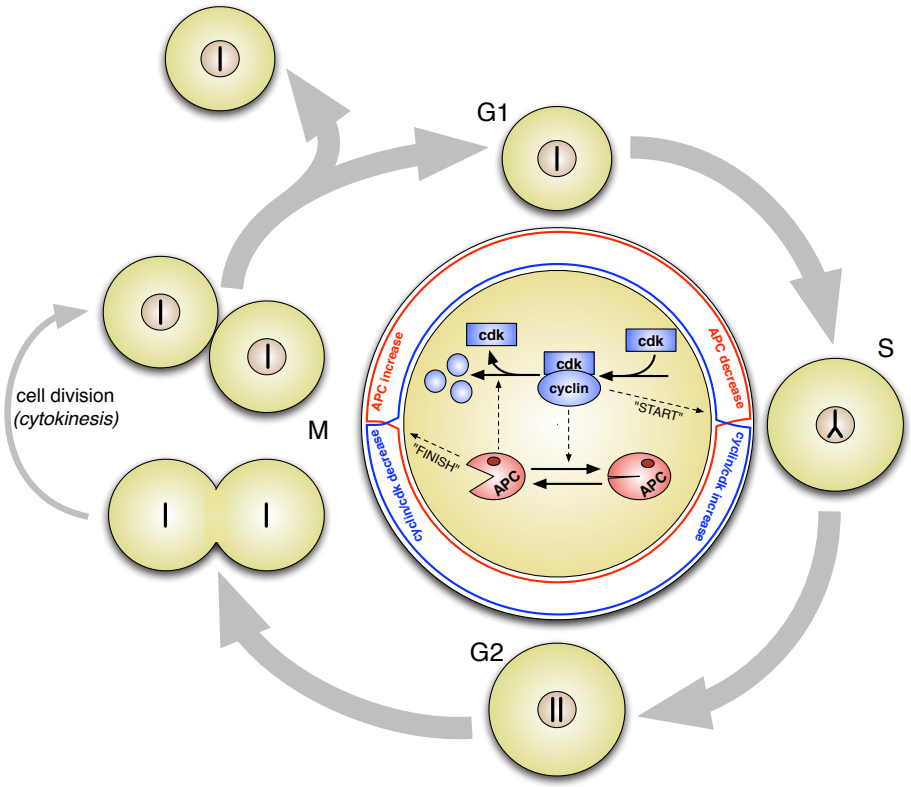

Figure 2.1: The cell cycle. The bistable loop between APC and Cyclin/Cdk is essential to establish a cell division cycle. The central cartoon of the molecular interactions between APC and Cyclin/Cdk was adapted from[76].

The picture we have drawn thus far is a huge simplification of the total cell cycle network as it is currently envisioned (see Figure 2.2)[51], here shown to illustrate the complexity of the network. The vastness of the network, as well as the richness of the behavior of even a small number of proteins necessitates

the use of mathematical models to quantitatively understanding regulation of the cell cycle.

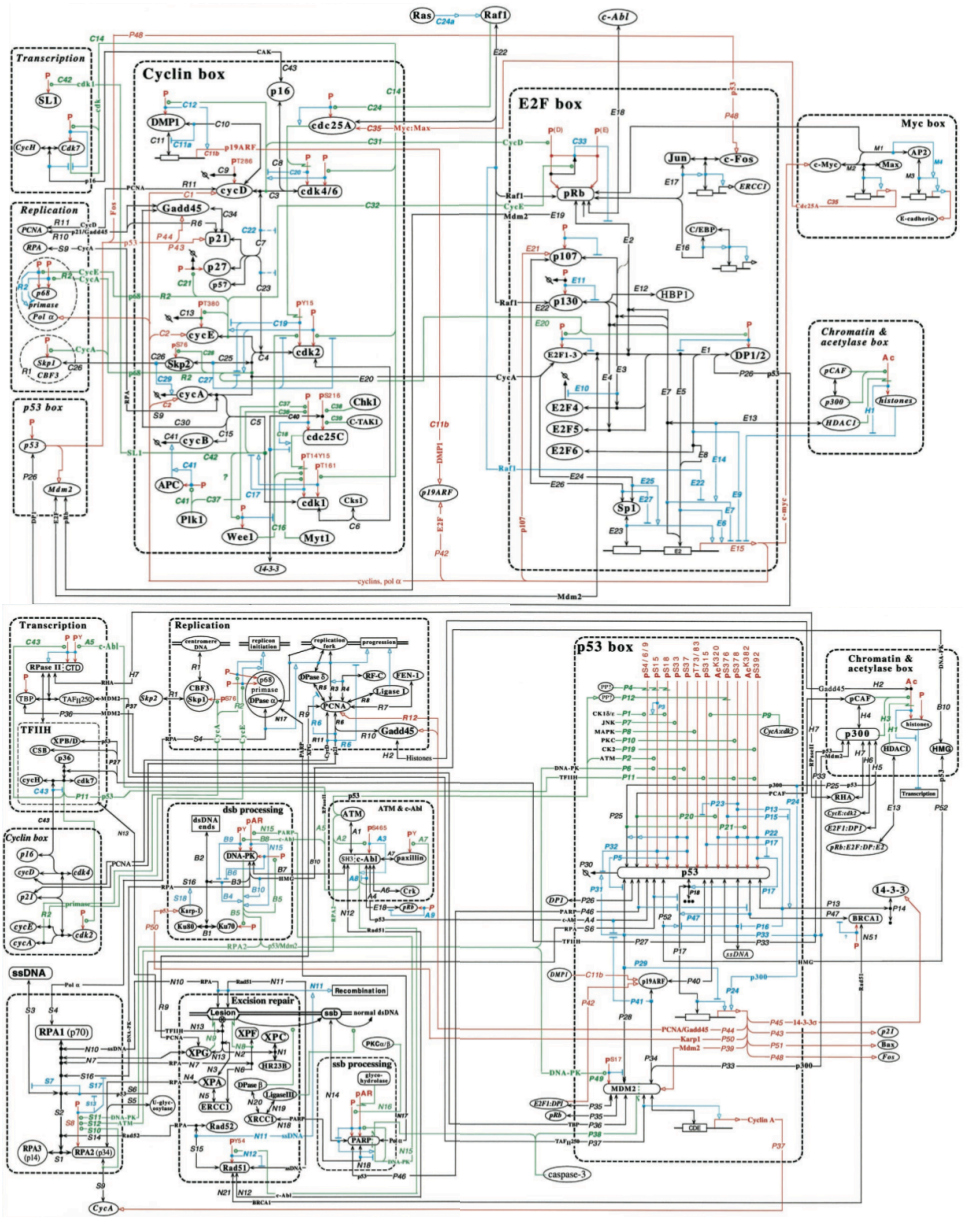

Figure 2.2: The mammalian cell cycle molecular interaction map as set out by Kohn[51].

2.2 Mathematical modeling of the cell cycle

Several research groups construct deterministic mathematical models of the eukaryotic cell cycle. Of these groups, Bela Novak's group from the University of Oxford and John Tyson's group from the Virginia Polytechnic Institute and State University are amongst the most active. Both these groups follow roughly the same methodology to construct their models - using ordinary differential equations (ODEs) to represent a minimal wiring diagram that, according to the current experimental knowledge, best describes the system under study. In this section we briefly introduce the methodology that is generally followed for the construction of cell cycle models described in terms of ordinary differential equations.

An ordinary differential equation describes how processes within a system affect the rate of change of a variable (X):

$$\begin{aligned}\{\text{rate of change of } X\} = \quad & \{ \quad \text{sum of rates of processes producing } X\} - \\ & \{ \quad \text{sum of rates of processes consuming } X\}\end{aligned}$$

or, more formally written as

$$\frac{dX}{dt} = \sum_{i=1}^{p} v_{production_i} - \sum_{i=1}^{c} v_{consumption_i} \tag{2.2.1}$$

where the rates of the processes v are summed for the total number (p) of reactions producing X substracted by the total number (c) of reactions consuming X.

The most predominant equations used to describe processes in the cell cycle are mass action kinetics (equation 2.2.2a), Michaelis-Menten kinetics (equation 2.2.2b) and Goldbeter-Koshland *zero-order ultrasensitivity* switches (equation 2.2.2c)[31,27].

Examples of rate equations used in cell cycle modeling:

$$v_{\text{mass action}} = k_1 A[t] B[t] \tag{2.2.2a}$$

$$v_{\text{michaelis-menten}} = \frac{V_{max} A[t]}{k_m + A[t]} \tag{2.2.2b}$$

$$\frac{d}{dt} X[t] = \frac{V_1 (X[t]_{tot} - X[t])}{K_1 + X[t]_{tot} - X[t]} - \frac{V_2 X[t]}{K_2 + X[t]} \tag{2.2.2c}$$

where in equation (2.2.2a), k_1 represents an elementary rate constant and $A[t]$ and $B[t]$ are two variable species that linearly affect the rate $v_{\text{mass action}}$. In equation (2.2.2b), used for enzyme catalyzed reactions, the rate $v_{\text{michaelis-menten}}$ is affected by a single specie, $A[t]$, and is dependent on two parameters - V_{max}, the maximum velocity of the reaction and K_M, the Michaelis constant which describes the affinity of the enzyme for its substrate. If an enzyme can exist in two different forms, of which only one is active, and if it displays abrupt switching between the two forms, a *zero-order ultrasensitivity* switch can be used to mathematically describe the switching behaviour. Assuming $X[t]$ is the active form, the equation can be expressed as equation (2.2.2c) where V_1 is the activation rate, V_2 is the inactivation rate and K_1 and K_2 are Michaelis constants.

Once a set of ODEs has been chosen to describe the wiring diagram of the cell cycle, an attempt is made to fit model parameters on experimental observations. If the set of ODEs fails to describe the experimental observations, the ODEs are adapted, followed by further parameter fitting until the set of ODEs can accurately describe the experimental observations of mutant and wild type cells. The most elaborate budding yeast cell cycle model currently available[14] for which this model construction method was used, is able to describe the phenotypic observations of 131 mutant strains.

2.3 Traditional Metabolic Control Analysis

Metabolic Control Analysis[48,38,40] is a mathematical framework that quantifies the dependencies of steady state properties such as flux or metabolite concentra-

tions on process activities. These dependencies are expressed in control coefficients, which can operationally be defined as the % change in a system property, X, upon a 1 % perturbation of a specific process activity, v_i. In mathematical terms:

$$C^X_{v_i} = \frac{\partial lnX}{\partial lnv_i} = \frac{\partial X/X}{\partial v_i/v_i} \tag{2.3.1}$$

An important property of control coefficients is that, for any flux, the control coefficients of all the processes within the system sum to unity (the **flux-control summation property**) and, for any concentration, the control coefficients of all the processes within the system sum to zero (the **concentration-control summation property**).

Expressed mathematically as:

$$\sum_{i=1}^{n} C^J_i = C^J_1 + C^J_2 + \ldots = 1 \tag{2.3.2a}$$

$$\sum_{i=1}^{n} C^x_i = C^x_1 + C^x_2 + \ldots = 0 \tag{2.3.2b}$$

The summation theorems illustrate that the control on a system property can be shared between the processes in a system. The ability to quantify the control of a process was a major improvement from the notion of a *rate-limiting step*.

In addition to showing that control exerted on a system property can be distributed between the system processes (refer to equation (2.3.2a)), MCA enables one to express the *systemic* control coefficients in terms of *local* properties. The **connectivity theorems** link the control coefficients to elasticity coefficients which can operationally be defined as the % change in a reaction rate, v_i, upon a 1 % perturbation of a parameter for the isolated reaction.

An elasticity coefficients can be expressed mathematically as:

$$\epsilon^{v_i}_x = \frac{\partial lnv_i}{\partial lnx} = \frac{\partial v_i/v_i}{\partial x/x} \tag{2.3.3}$$

We do not go in great detail on the applications of elasticity coefficients as they do not play an important role in the MCA for dynamic systems as treated in this thesis.

2.4 Metabolic Control Analysis for dynamic systems

Metabolic Control Analysis (MCA) is mostly used to analyze time invariant properties of steady state systems. However, dynamical systems exhibit both time dependent and time independent behaviour. Examples of time dependent system properties for dynamic systems are reaction rates and metabolite concentrations, which vary with time (for instance in an oscillatory system), while time independent system properties such as oscillation frequency are constant in the limit cycle.

Several extensions to MCA have been made to analyze the control on time independent system properties of oscillatory systems such as frequency, average value, amplitude, waveform, phase shift, period, local minima, and local maxima[8,49,22,61,63,62,47,45].

MCA for time dependent system properties has been made by[44] for which time dependent control coefficients were used, which are not useful for the analysis of the cell cycle. The control analysis of the cell cycle, and specifically its time dependent properties are important for the work presented in this thesis. In Chapter 3, we will treat in detail our extension to MCA for these systems.

Chapter 3

Summation theorems for flux and concentration control coefficients of dynamic systems*

3.1 Abstract

Metabolic Control Analysis (MCA) was developed to quantify how system variables are affected by parameter variations in a system. In addition, MCA can express the global properties of a system in terms of the individual catalytic steps, using connectivity and summation theorems to link the control coefficients to the elasticity coefficients. MCA was originally developed for steady state analysis and not all summation theorems have been derived for dynamic systems. A method to determine time-dependent flux and concentration control coefficients for dynamic systems by expressing the time domain as a function of percentage progression through any arbitrary fixed interval of time is reported. Time-dependent flux and concentration control coefficients of dynamic systems, provided that they are evaluated in this novel way, obey the same summation the-

*The work presented in this chapter was published: Conradie, R; Westerhoff H V; Rohwer J M; Hofmeyr J H S; Snoep J L (2006) Summation theorems for flux and concentration control coefficients of dynamic systems. IEE Proc. Syst. Biol. 153(5): 314-7.

orems as steady-state flux and concentration control coefficients, respectively.

3.2 Introduction

MCA is a theoretical framework that was initiated by Kacser and Burns[48] and Heinrich and Rapoport[38,39]. One motivation was to quantify how system variables (such as concentrations of metabolites and fluxes through a metabolic pathway) change in response to parameter variations (perturbations) such as changes in enzyme concentrations. A further motivation for developing MCA was to describe the global regulatory properties of a system of reactions in terms of properties of the individual catalytic steps. These goals have been achieved in the form of control, elasticity and response coefficients as well as summation and connectivity theorems. Traditionally control coefficients quantify the change that a steady state variable, such as flux and concentration, undergoes when a small change is made to the activity of an independent process step in the system. Elasticity coefficients, on the other hand, quantify to what extent the rate of an independent process in a system is changed immediately upon a change of any molecular species or parameter that affects that process directly. The relations between these coefficients are given by the summation and connectivity theorems, which make it possible to express the systemic regulatory properties in terms of the characteristics of the individual steps[48,38,39], thereby making MCA an ideal tool for system biologists. In accordance with the summation theorem, numerous ideas regarding metabolism, such as the existence of a rate-limiting step in a metabolic pathway have been replaced with a rigorous quantitative description, e.g. the control of a pathway is distributed among the different catalytic steps of the pathway.

MCA has been implemented successfully *vis-à-vis* many metabolic systems that exhibit steady state behaviour. Traditional MCA was not able to describe dynamical systems where temporary or permanent variations of metabolic fluxes and concentrations are significant. Advances in experimental techniques and the realization that many cellular mechanisms can only be understood on the basis

of their dynamical behaviour have led to an increase in the number of investigations of dynamical systems (i.e. calcium waves, neuronal signal oscillations, cAMP oscillations, signal transduction pathways and the cell cycle). Therewith, the potential assets of a method that can contribute to our understanding of dynamical systems in ways similar to the ways in which MCA has contributed to understanding steady-state systems, have become more evident.

One of the first extensions to traditional MCA, so that it can describe dynamical systems, was to introduce a time-dependent control coefficient[3]. Unfortunately this formulation could not be generalized to all dynamical systems as it does not appear to be very useful for describing autonomously oscillating systems because the magnitude of the time-dependent control coefficient diverges as time progresses[49,22]. Acerenza and Kacser[2,1] then analysed the control properties of time-invariant variables with dimensions of time (i.e. relaxation time and period of oscillation) of time-dependent systems by MCA and also deduced summation theorems for them. Unfortunately the variables traditionally analyzed with MCA in steady state systems (i.e. fluxes and concentrations) are not just time-invariant variables with dimensions of time and hence cannot be determined as proposed by Acerenza and co-workers. Also, extensions to standard MCA proposed by Heinrich and Reder[41] cannot be generalized to all dynamical systems because concentrations of metabolites are not necessarily in the vicinity of a steady state[49,22]. As a result, MCA-like approaches for time independent variables of autonomously oscillating systems such as frequency, amplitude, average value, waveform, phase shift[49,22,80,8,61,63] and for signal transduction pathways (i.e. signal maximum (amplitude), its ultimate value (final strength), its duration and its time-integrated concentration) have been performed[44]. A formal mathematical description of sensitivity analysis on extrema and period of autonomously oscillating systems has been developed[45].

It has hitherto not been possible to quantify the control that each reaction step of a dynamical system plays in regulating fluxes and metabolite concentrations. In this contribution we show how time-dependent flux and concentration control coefficients can be determined for dynamical systems when the time domain is treated as percentage progression through any arbitrary fixed interval of time.

Furthermore, we show that steady state flux and concentration control summation theorems also hold for dynamical systems. Lastly, we illustrate the approach using a kinetic model of a system with temporary variations (a signal transduction model) as well as a system with permanent fluctuations (an autonomously oscillating system).

3.3 Methods

The work of Acerenza and coworkers[3,2,1] has shown that upon multiplication of all rate equations of a system (β) with a constant factor (d) the new system (β_d) can be described as a function of β. This corresponds to a time transformation from $t = 0$ onwards[22,44]. The time dependence of the state variables in β_d, $s_d(t)$, can be expressed as a function of the state variables in $\beta(s(t))$ as follows:

$$s(t) = s_d(t/d) \tag{3.3.1}$$

Any time point (t) in an arbitrary fixed length of time (T) between time t_0 and time $t_0 + T$ can be expressed as:

$$t = t_0 + t_1, t_1 = 0, ..., T \tag{3.3.2}$$

with:

$$t_1 = zT, z = 0, ..., 1 \tag{3.3.3}$$

where z is the fraction of progression through the interval, i.e. the *phase* $[t_0, t_0 + T]$.

Combining equations 3.3.1, 3.3.2 and 3.3.3 we obtain:

$$s(t_0 + zT) = s_d((t_0/d) + z(T/d)) \tag{3.3.4}$$

Thus, the concentration of any metabolite at a certain percentage progression through one arbitrary fixed interval of time in system β would be the same as the concentration of that metabolite in system βd at the same percentage progression (at the same phase). Furthermore, since the metabolite concentrations at the same percentage progression are constant, the fluxes will increase proportionally with d (the multiplier of the reaction rates).

This implies that, when expressing the time domain as a function of percentage progression through an arbitrary fixed time interval, time dependent concentration control coefficients and time dependent flux control coefficients sum to 0 and 1 respectively at any percentage progression through that interval. This proof is valid for systems engaging in regular oscillations, i.e. repetitions with time independent period T. For the proof for transient conditions we define T so as to correspond to a point in time with a certain magnitude of a variable X_i. Then the proof proceeds further as above, with the difference that z may exceed 1.

It is crucial that the control coefficients used here are evaluated in a special way: the activity of any process i is increased by $p\%$ and the new concentration is read $p\%$ earlier. This is then repeated for all processes, and the results are summed over all processes. In this sense the control coefficients defined here are not standard control coefficients. For these, the effect of the $p\%$ change in enzyme activity is read at the same time. Then, then at least for transients the sum of the concentration control coefficients should not equal zero but the time control coefficient[44].

To illustrate the approach, MCA was performed on the oscillatory phosphofructokinase (PFK) model developed by Goldbeter and coworkers[32,30] as well as on a kinetic model exemplifying the mechanisms of signal transduction constructed by Hornberg *et al.*[44].

3.4 The models

3.4.1 A dynamical system with permanent variations with time

The phosphofructokinase (PFK) model developed by Goldbeter and coworkers[32,30], is a core model that describes the dynamic behaviour of glycolysis in terms of the kinetics of the enzyme PFK. The model can be accessed and run on JWS Online (http://jjj.biochem.sun.ac.za/database/goldbeter/index.html). The variables $\alpha[t]$ and $\gamma[t]$ denote the substrate concentrations (fructose 6-phosphate or ATP) and product concentrations (fructose 1,6-bisphosphate) respectively. Reaction 1 denotes the constant injection rate of substrate and reaction 3 the constant rate of product removal. Reaction 2 encapsulates the most important kinetic details of PFK along with the rate constant (or enzyme concentration).

3.4.2 A dynamical system with transient variation

The kinetic model by Hornberg *et al.*[44] was constructed to elucidate the principles governing the control of signal transduction. The model represents a simple linear pathway that consists of a receptor and three consecutive kinase/phosphatase monocycles. The model represents a simplified MAP kinase pathway where the active receptor R (activated by reaction 1) phosphorylates (activates) X1 to X1P. In turn, X1P acts as a kinase by phosphorylating X2 to X2P. X2P then finishes the three step phosphorylation by activating X3 to X3P. These phosphorylation steps are denoted by reactions 3, 5 and 7. Reaction 2, 4, 6 and 8 encapsulates the phosphatase reactions recycling the active species back to Ri, X1, X2 and X3. The authors used signal amplitude A (i.e. the maximum concentration of X3P attained) and the duration of signalling b (i.e. the time point where the concentration of X3P dropped below an arbitrary threshold value of 5% of total X3 (=0.05)) to perform their analyses. This model can be viewed and run on JWS Online (http://jjj.biochem.sun.ac.za/database/Hornberg/index.html).

3.5 Results and Discussion

3.5.1 A dynamical system with permanent fluctuations

Time simulations for the PFK model with variables $\alpha[t]$ and $\gamma[t]$ and time simulation of the same PFK model but with all the rates multiplied by the same arbitrary constant d ($d = 0.95$) with variables $\alpha_d[t]$ and $\beta_d[t]$ are shown in Fig. 3.1.

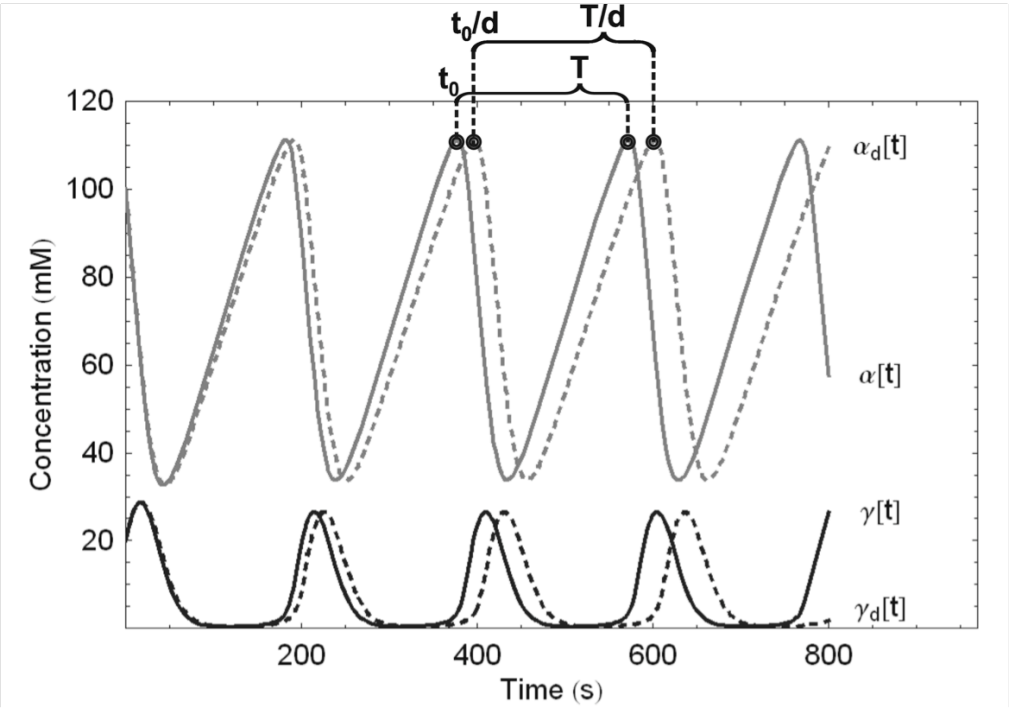

Figure 3.1: Time simulations of the PFK model (solid lines) with variables $\alpha[t]$ and $\gamma[t]$ and the same PFK model but with all the rates multiplied by the same arbitrary constant d (dashed lines) with variables $\alpha_d[t]$ and $\gamma_d[t]$.

Fig. 3.1 shows that the amplitude of $\alpha[t]$ and $\alpha_d[t]$ are equal, as are the amplitudes of $\gamma[t]$ and $\gamma_d[t]$, which is in agreement with the summation theorem for amplitude. In addition, the frequency of the system is changed with a constant factor d. This is in agreement with the summation theorem for frequency. t_0 and T are time invariant properties of the system with dimensions of time. When multiplying all rate equations by a factor d they transform into (t_0/d) and

(T/d) respectively[2,1] (see Fig. 3.1). Even though these two systemic parameters are scaled by d, the concentrations of metabolites in both systems are identical when compared at the same percentage progression (z) through $[t_0, t_0 + T]$, i.e. $\alpha[t] = \alpha_d[t/d]$ and $\gamma[t] = \gamma_d[t/d]$.

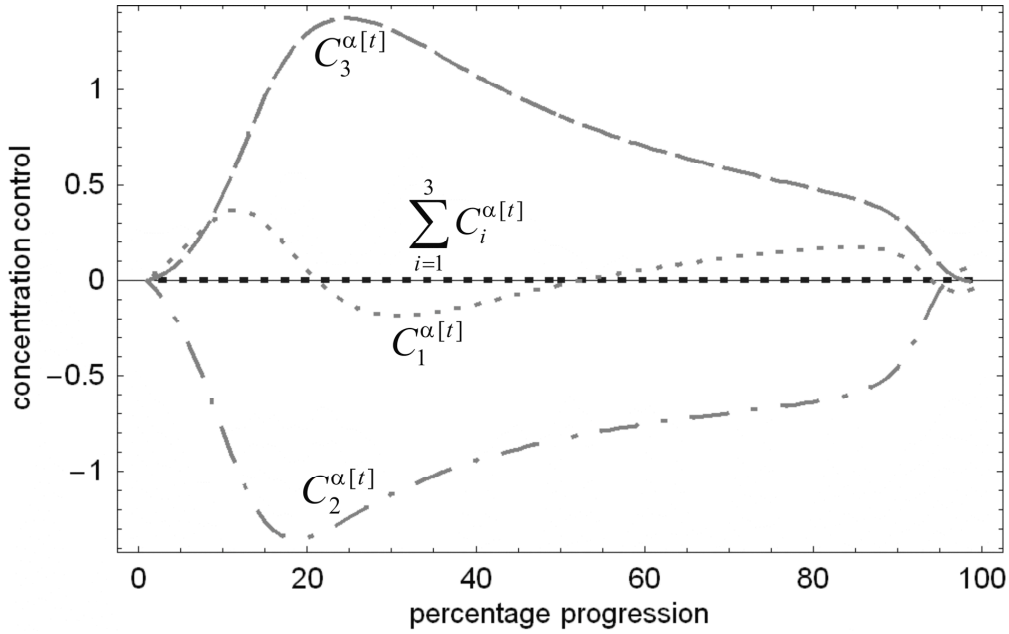

Figure 3.2: Concentration control coefficients ($C_1^{\alpha[t]}$, $C_2^{\alpha[t]}$, $C_3^{\alpha[t]}$) and the sum of these control coefficients, $\sum_{i=1}^{3} C_i^{\alpha[t]}$, as a function of percentage progression through one oscillatory period.

This method was used to perform a control analysis on the PFK oscillatory system. Results obtained from this analysis are depicted in Fig. 3.2 and Fig. 3.4. The control analysis, for which the time domain is expressed as a function of percentage progression through one period, confirmed that the steady state summation theorem for concentration control coefficients ($\sum_{i=1}^{n} C_i^S = 0$) also holds for oscillatory systems (Fig. 3.2). Similarly, it can be seen from Fig. 3.3 that the steady state summation theorem for flux control coefficients also holds for oscillatory systems i.e. $\sum_{i=1}^{n} C_i^J = 1$.

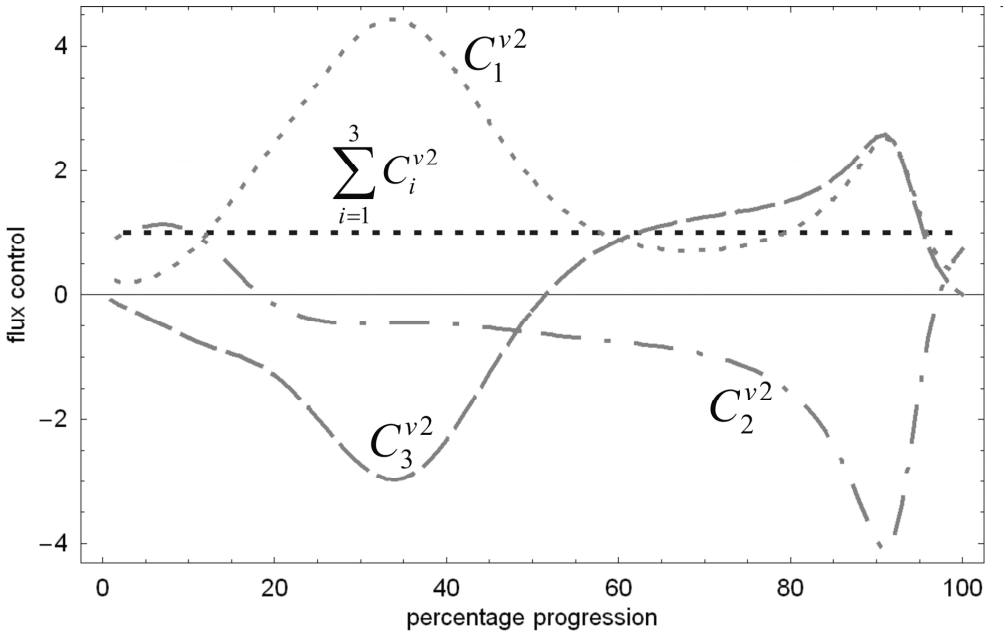

Figure 3.3: Flux control coefficients (C_1^{v2}, C_2^{v2}, C_3^{v2}) and the sum of these control coefficients, $\sum_{i=1}^{3} C_i^{v2}$, as a function of percentage progression through one oscillatory period.

3.5.2 A dynamical system with transient variation

The signal transduction model constructed by Hornberg *et al.*[44] was used to determine the control that the respective processes exert on signalling amplitude of X3P (A), duration (b) of signalling (i.e. when X3P reaches a concentration of 0.05), the integral of X3P over time (i.e. the area under X3P until it reached b) and the final signalling amplitude (i.e. the concentration of X3P at steady state)[44]. A simulation of this model and the values of A and b can be seen in Fig. 3.4.

MCA was performed to determine the time dependent concentration and time dependent flux control coefficients. The arbitrary fixed interval of time selected to perform our analyses had a lower bound of zero and an upper bound of time b where X3P reaches a threshold value of 5% of total X3 (=0.05). Hornberg *et al.*[44] grouped the various reactions into two functional groups called activating processes (reactions 2, 3, 5 and 7) and deactivating processes (reactions 1, 4, 6

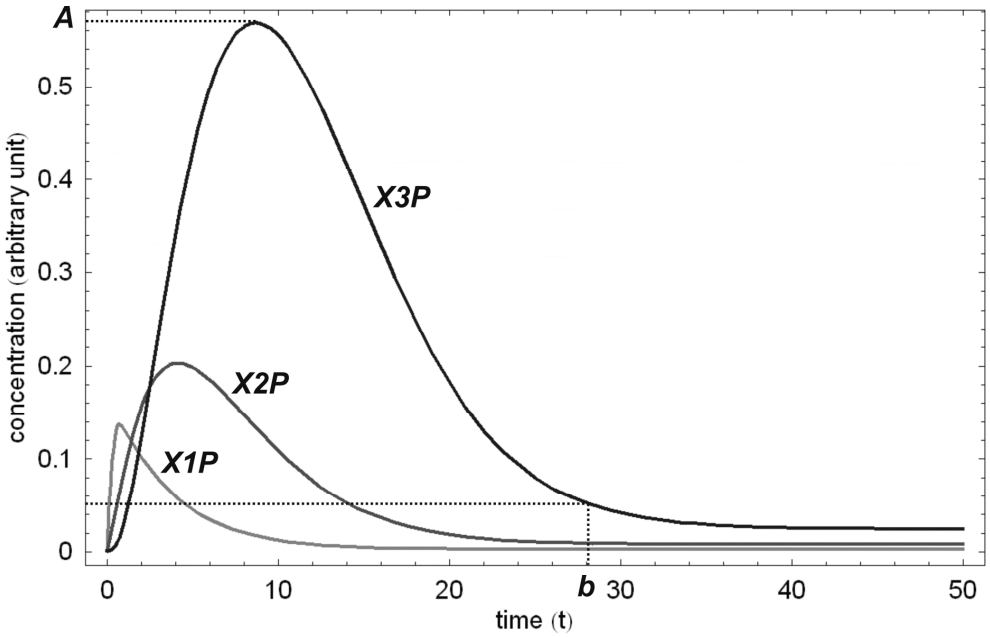

Figure 3.4: Time course of the signal transduction model constructed by Hornberg *et al.* The varying concentrations of metabolites X1P, X2P and X3P are shown along with the maximum concentration value (A) reached by metabolite X3P. The time (b) at which X3P reaches an arbitrary value of 0.05 is also shown.

and 8). We also used the same grouping and calculated the control the activating processes have on the flux from X3 (inactive signalling molecule) to X3P (active signalling molecule) and the control the deactivating processes have on the same flux. The time course of these two control coefficients, $C^{v7}_{activators}$ and $C^{v7}_{deactivators}$, as well as $\sum_{i=1}^{8} C_i^{v7}$ are shown in Fig. 3.5.

Our analyses show that the control of flux from X3 (inactive signalling molecule) to X3P (active signalling molecule) is, at the beginning of the signal, controlled by the kinases. However, at a higher percentage progression, the control exerted on the flux by the activating processes decreases. The signalling system then momentarily reaches a state where both the activating and deactivating processes have the same control over flux v7. When approaching time point b the control on the flux that creates active signalling molecules is taken over by the deactivating reactions until the signal is dissipated.

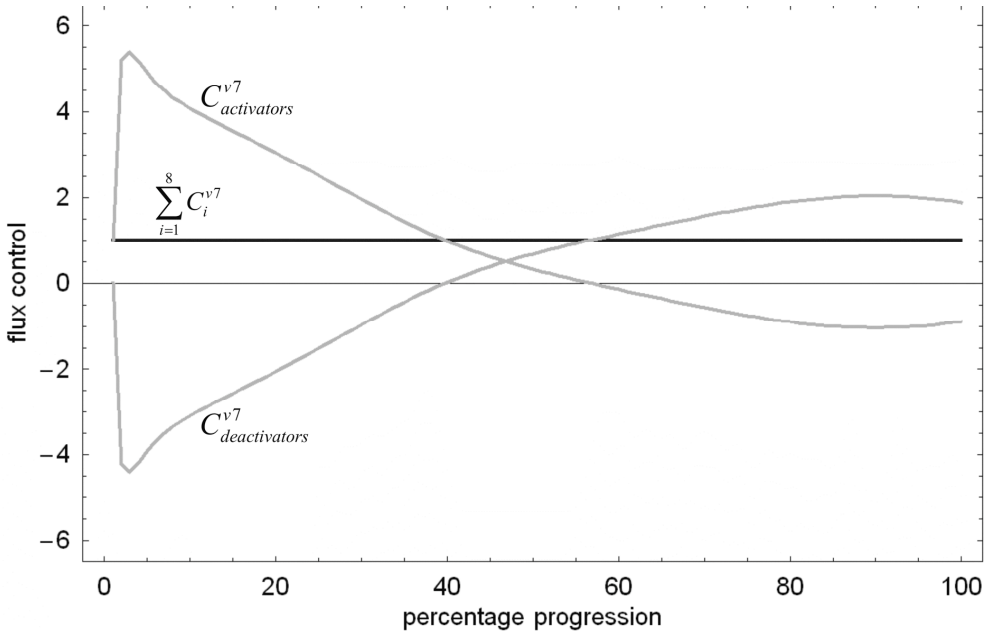

Figure 3.5: Flux control coefficients of activators and deactivators($C^{v7}_{\text{activators}}$ and $C^{v7}_{\text{deactivators}}$) and the sum of all control coefficients on rate v7, $\sum_{i=1}^{8} C_i^{v7}$, as a function of percentage progression through the interval $[0, b]$. b is the time where the concentration of $X3P$ reaches a value of 0.05.

3.6 Conclusion

We have developed a method, based on the expression of time as a function of percentage progression of a chosen time interval, for MCA of dynamic systems. Using the method, we could show that the same summation theorems that hold for concentration control coefficients and flux control coefficients of steady-state systems also hold for dynamic systems. The generic method developed in this article has been used to analyse a range of autonomously oscillating systems, regardless of whether the oscillations are of a continuous or a discontinuous nature. Furthermore, our method not only works for dynamic systems with sustained variations (oscillations) but also for dynamic systems with transient variations such as in signal transduction.

3.7 Acknowledgements

R.C. acknowledges generous support from the National Bioinformatics Network (South Africa) and thanks Franco du Preez for intensive discussions. H.W. thanks Boris Kholodenko and Frank Bruggeman for many discussions.

3.8 Proof of the relationship between progression control coefficients and time-dependent control coefficients

The proof set out here was a contribution made by us in the Journal of Mathematical Biology[82]. In the progression control coefficient the perturbation of the phase of the response is corrected for by determination of the control coefficients at a given progress point (corresponding to the phase in a periodic phenomenon). That perturbation of phase is the essence of the time control coefficients. The relation between the two types of control coefficients can be described as:

$$C_j^{c_i(t)} = C_j^{c_i(pA)} - C_t^{c_i(t)} C_j^A \tag{3.8.1}$$

where the control by reaction j on the concentration c_i at a fixed time point t is expressed as a function of the concentration control by j at a point in the progress curve corresponding to t (i.e. pA) and the control by time on the concentration, multiplied by the control of reaction j on the length of the progress curve (A). The latter control measures the extent to which the modulation of reaction j stretches (retards) the time dependence of the process.

The analysis is valid for any type of dynamic behavior and the point A can be set as a threshold of a concentration but can also be the maximum of a periodic signal. One of the advantages of using the progression control analysis is that it is not sensitive to the growing dispersion between the original and the perturbed

signal, which is especially important for analyses over a prolonged time period, for instance when analyzing a periodic signal.

Summation of equation 3.8.1 over all the reaction steps yields:

$$\sum_{j=1}^{n} C_j^{c_i(t)} = \sum_{j=1}^{n} C_j^{c_i(pA)} - C_t^{c_i(t)} \sum_{j=1}^{n} C_j^{A} \tag{3.8.2}$$

with

$$\sum_{j=1}^{n} C_j^{A} = -1 \tag{3.8.3}$$

and

$$\sum_{j=1}^{n} C_j^{c_i(pA)} = 0 \tag{3.8.4}$$

which reduce Eq. 3.8.2 to

$$0 = -C_t^{c_i(t)} + \sum_{j=1}^{n} C_j^{c_i(t)} = 0 \tag{3.8.5}$$

Eq. 3.8.5 is the time dependent summation law for concentration control coefficients[44]. This shows that correction for the phase-shift renders the classical summation theorem. Below a more detailed proof for the relationship between progression control coefficient and time-dependent control coefficient is given[†] (Figure 3.6 is a figure to aid in explaining the proof):

A time-dependent control coefficient is defined as,

$$\delta \ln x(t, v_j) = \frac{\partial \ln x}{\partial \ln v_j}(t, v_j)\delta \ln v_j = C_j^x(t)\delta \ln v_j \tag{3.8.6}$$

[†]Extended proof was derived by Frank J. Bruggeman.

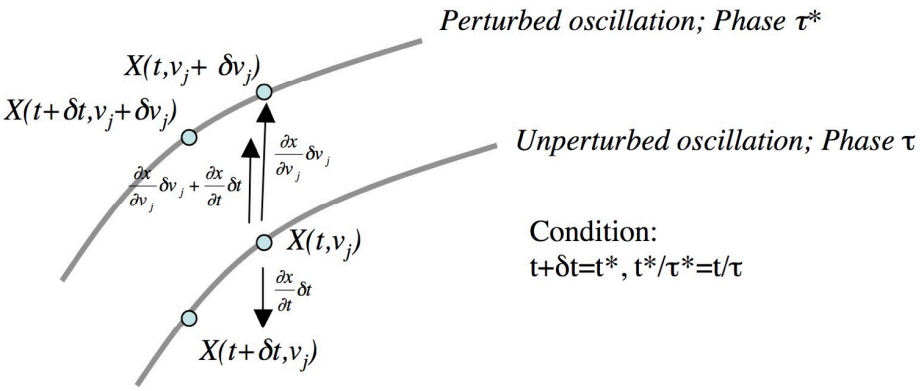

Figure 3.6: A geometrical interpretation of the proof set out below; The time course for the unperturbed oscillation; Phase τ and the perturbed oscillation; Phase τ^*.

It corresponds to the difference in a state variable between a perturbed and an unperturbed system.

The progression control coefficient is defined for oscillatory systems at a time point for the perturbed system that correspond to an equal progression along the oscillation (phase, t/τ; with τ as period). If we define $t + \delta t$ as the correct time in the perturbed network, such that it has the same phase as the unperturbed system, then we obtain,

$$\delta \ln x(t + \delta t, v_j) = \frac{\partial \ln x}{\partial \ln v_j}(t, v_j)\delta \ln v_j + (\frac{\partial \ln x}{\partial \ln t}(t, v_j))_{\tau fixed}\delta \ln t \qquad (3.8.7)$$

Thus for the perturbed system, we have as the reference time $t + \delta t = t^*$ and phase τ^*. δt has been chosen such that $t/\tau = t^*/\tau^*$; to ascertain such that the phase is preserved,

$$\delta \ln t = \delta \ln \tau = \frac{\partial \ln \tau}{\partial \ln v_j}\delta \ln v_j \qquad (3.8.8)$$

The progression control coefficient $C_j^{x(t-\delta t)}$ is defined as:

$$\delta \ln x(t+\delta t, v_j) = (\frac{\partial \ln x}{\partial \ln v_j}(t, v_j) + \frac{\partial \ln x}{\partial \ln t}(t, v_j)\frac{\partial \ln \tau}{\partial \ln v_j})\delta \ln v_j \quad (3.8.9)$$

$$= (C_j^x(t) + C_t^x(t)C_j^\tau)\delta \ln v_j \quad (3.8.10)$$

$$= C_j^{x(t+\delta t)}\delta \ln v_j \quad (3.8.11)$$

Therefore,

$$C_j^{x(t+\delta t)} = C_j^x(t) + C_t^x(t)C_j^\tau \quad (3.8.12)$$

$$\implies C_j^x(t) = C_j^{x(t+\delta t)} - C_t^x(t)C_j^\tau \quad (3.8.13)$$

Equation 3.8.13 corresponds to equation 3.8.1 also described in the Journal of Mathematical Biology[82].

Given

$$\sum_{j=1}^{n} C_j^{x(t+\delta t)} = \sum_{j=1}^{n} C_j^x(t) + C_t^x(t)\sum_{j=1}^{n} C_j^\tau \quad (3.8.14)$$

and since

$$\sum_{j=1}^{n} C_j^\tau = -1 \quad (3.8.15)$$

$$\sum_{j=1}^{n} C_j^x(t) = \frac{d \ln x}{d \ln t} = C_t^x(t) \quad (3.8.16)$$

we obtain for the summation theorem:

$$\sum_{j=1}^{n} C_j^{x(t+\delta t)} = C_t^x(t) - C_t^x(t) \cdot 1 = 0 \quad (3.8.17)$$

Chapter 4

Restriction Point Control of the Mammalian Cell Cycle via the Cyclin E/Cdk2:p27 Complex *

4.1 Summary

Numerous kinetic models, employing a mixture of top-down and bottom-up approaches, have been constructed to describe the cell cycle. These models have typically been constructed, validated and analyzed using model species (molecular intermediates and proteins) and phenotypic observations, and therefore do not exclusively focus on the individual model processes (reaction steps). We have developed a method to: 1) quantify the importance of each of the reaction steps in a kinetic model for the positioning of a switch point (here the restriction point); 2) relate this control of reaction steps to their effects on molecular species, using sensitivity and co-control analysis; and thereby 3) go beyond a correlation towards a causal relationship between molecular species and effects.

*The work presented in this chapter was accepted for publication: Riaan Conradie, Frank J. Bruggeman, Andrea Ciliberto, Attila Csikász-Nagy, Bela Novák, Hans V. Westerhoff, Jacky L. Snoep (August 2009) Restriction Point Control of the Mammalian Cell Cycle via the Cyclin E/Cdk2:p27 Complex. FEBS Journal.

The method is generic and can be applied to responses of any type but is most useful for the analysis of dynamic and emergent responses such as switch points in the cell cycle. The strength of the analysis is illustrated for an existing mammalian cell cycle model focusing on the restriction point (RP)[56].

The reactions in the model with the highest RP control were those involved in: 1) the interplay between retinoblastoma protein (Rb) and E2F transcription factor; 2) those synthesizing the delayed response genes (DRG) and Cyclin D/Cdk4 in response to growth signals; 3) the E2F dependent Cyclin E/Cdk2 synthesis reaction, as well as 4) p27 formation reactions. Nine of the 23 intermediates were shown to have a good correlation between their concentration control and RP control. Sensitivity and co-control analysis indicated that the strongest control of RP is mediated via the Cyclin E/Cdk2:p27 complex concentration. Any perturbation of the RP could be related to a change in the concentration of this complex; apparent effects of other molecular species were indirect and worked always through Cyclin E/Cdk2:p27, indicating a causal relation between this complex and the positioning of RP.

4.2 Introduction

Arthur Pardee[58] defined the restriction point (RP) as the apparent switch point in the late G1 phase, beyond which normal cells would only progress when supplied with a sufficient, mitogen containing culture medium. Once the cell has transgressed the RP, the necessity of a mitogen (i.e. growth factor) containing medium was relieved and cells will commit to replicate their DNA (S-phase) and complete the remainder of the division cycle autonomously[60,9]. Cells in the G1-phase that have not yet passed RP, monitor their environment and own size to determine whether they are ready to commit to S-phase entry and division cycle completion or, in contrast, enter the resting G0-phase[60], where most non-cancerous somatic mammalian cells spend their lifetime. Disregulation of the RP has been linked to several disease states, most notoriously cancer[58,84], and quantification of the contribution of the different reaction steps in the cell cycle

to the control of the RP would be important for drug target identification studies and for understanding the action mechanism of existing, RP affecting drugs.

Abrupt cell cycle transitions (e.g. G1/S) are properties of the complete underlying control system which can be described without the necessity to introduce hypothetical regulatory proteins or hard code a decision event[56,7]. Numerous kinetic models that incorporate the existing knowledge of the molecular mechanism of the restriction point have been constructed[36,56,4,33]. Novak and Tyson[56] constructed their kinetic model on the RP of the mammalian cell cycle using a yeast-like core model of the cyclin-Cdk interactions (emphasizing the deep similarities of the yeast and mammalian cells Cdk-regulatory system). They extended this core model with kinetic modules for the growth factor sensing machinery of mammalian cells; the retinoblastoma and E2F transcription factor interactions and the antagonism between the cyclin-dependent kinase inhibitor, ($p27^{Kip1}$), and Cyclin A/Cdk2 and Cyclin E/Cdk2. With their kinetic model, Novak and Tyson could account for the Zetterberg and Larsson experiments, which proved the existence of RP and positioned it somewhere in the G1 phase[85]: (i) cells pulse treated (1h) with cycloheximide early in the cell cycle (before RP) immediately suffer a long delay in the cell division cycle, (ii) cells treated late in the division cycle finish the current cycle similar to untreated cells but are significantly delayed in the subsequent division cycle and (iii) cells treated directly after the restriction point do not suffer any delays in the current or subsequent division cycles.

Kinetic models that are constructed on the basis of known biochemical information about the system and its components, are routinely used to integrate this knowledge and compare the resulting simulations with experimental observations. More extensive analysis methods are necessary to quantify the importance of each of the reaction steps for the systemic behavior. Metabolic Control Analysis (MCA)[48,38] is a rigorous framework that enables one to assess how a biological function is controlled by the various molecular processes in the cell sustaining that function. MCA has been used predominantly to analyse the control distribution in steady states, although the theory has been generalised for systems with dynamic behavior[63,47,49,22,19]. In this contribution we develop and

implement an extension to MCA that can be used not only to quantify the control of system variables, but also to infer via which molecular species this control was elicited.

Our approach is well suited for systems biology studies where the primary goal is to come to a quantitative understanding of systemic properties (such as the emergent restriction point in the mammalian cell cycle) in terms of the multitude of reaction steps and interactions between the cell's molecular parts (such as cell cycle proteins)[68]. Numerous researchers have recognised the need for theoretical approaches in molecular biology[54,34,53,57,29,52]. Our novel framework would be useful for molecular and systems biologists to determine which reactions exert important control on a high-level system property, and explain via which molecular species these reaction steps exert control.

Applying our approach to the RP, as modeled in the kinetic model developed by Novak and Tyson[56], revealed that the control of RP was distributed over the different reaction steps in the network. The highest control was exerted by the reactions responsible for: 1) the interaction between retinoblastoma protein (Rb) and E2F transcription factor; 2) synthesis of DRG and Cyclin D/Cdk4 in response to growh signals; 3) the E2F dependent Cyclin E/Cdk2 synthesis reaction; and 4) the p27 formation reactions. In addition, our analysis revealed that RP control was exerted via the Cyclin E/Cdk2:p27 complex. Independent of which reaction step or which molecular species was perturbed, all effects on the restriction point could be explained via an effect of the perturbation on Cyclin E/Cdk2:p27.

4.3 Model, Methods and Theory

The model presented by Novak and Tyson[56] consisted of 18 ordinary differential equations (ODEs) and several algebraic equations. Each of these ODEs were used, along with the wiring diagram of the mammalian cell cycle network, to distil 52 reaction steps from the network such that each step formed a functional unit within the network. The retinoblastoma and E2F transcription factor in-

teractions which were coded as steady state algebraic equations in the original model were coded explicitly as ODEs, increasing the number of ODEs to 23 (see Appendix 1). The reaction network of the cell cycle model is schematically represented in Figure 4.1.

Mathematica 6.0 was used for all simulations. The ODEs were solved using the NDSolve function in combination with the EventLocator method to precisely locate events during the simulation. A simulation result in which the restriction point and the different phases of the cell cycle are indicated, is shown in Figure 4.2.

MCA is a theoretical framework that can be used to calculate the importance of each of the steps in a reaction network for the systemic behavior, using so-called control coefficients[48,38]. We used a perturbation method for calculating control coefficients by adding a multiplier to each of the 52 steps (α_1 to α_{52}) and perturbing each reaction individually (0.1 per million perturbation up and down). After each perturbation the model was simulated until a new limit cycle was reached and then control coefficients for stationary behavior, e.g. position of RP or the length of the G_1 phase, were calculated and expressed as a fraction of the cell division cycle. For non-stationary behavior (i.e. time dependent variables such as concentrations of metabolites or flux values for reaction steps) an extension of MCA was used that enables the determination of control coefficients as the system progresses through an arbitrary fixed interval of time (e.g. the cell division cycle), for a detailed description of the method see[19] (Chapter 3 in this thesis).

Results and Discussion

Control of the Restriction Point

We used a perturbation method to quantify the control of the respective reaction steps in a mammalian cell cycle model on the time of occurrence of the restriction point, C_i^{RP}. The analysis revealed (Figure 4.3) that the control is distributed

over the reaction network with the majority of the reactions steps exerting a small to moderate control ($|C_i^{RP}| < 1$). Eight reaction steps exerted a high control ($|C_i^{RP}| > 2$) on the restriction point; four of which caused a delay (positive control) while the others advanced the restriction point (negative control). The C_i^{RP} for all reaction steps sums up to 0, this is to be expected on the basis of our definition of RP as a fraction of the cell division cycle. The control coefficient of reaction step x on RP is the percentage change in the fraction of the cell cycle length at which RP occurs for a 1% change in the activity of x. If we had defined the RP as an absolute time point, then the sum of control coefficients would add up to -1 (as they do for the control on the cell division time).

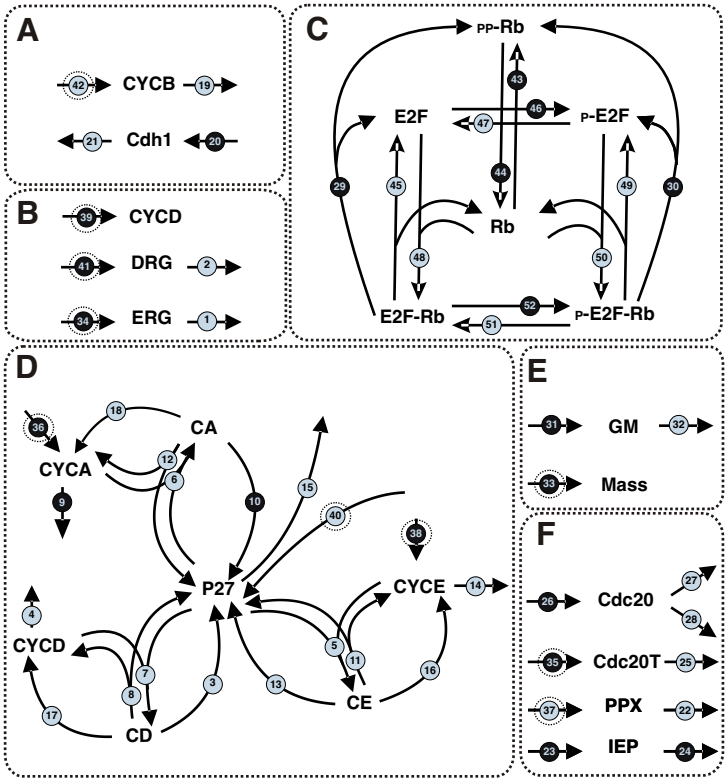

Figure 4.1: The reaction network scheme of the mammalian cell cycle model. The network consists of 52 reactions which are grouped into 6 modules. A.) A central component of the model is the antagonism between Cyclin B and Cdh1 (reactions 19, 20, 21 and 42). This antagonistic nature of the cell cycle is found amongst all eukaryotes. B.) Included in the mammalian cell cycle model are the early and delayed-response genes (ERG and DRG respectively). In the scheme the steps responsible for ERG, DRG and Cyclin D synthesis are reactions 34, 39 and 41. Growth factors bind to specific receptors found on the plasma membrane to subsequently stimulate an intracellular signal-transduction pathway that activates ERGs. The ERGs then activate DRGs and Cyclin D which set the cell division cycle in motion. C.) The retinoblastoma protein (Rb) is a general inhibitor of E2F (a transcription factor), and is distributed between an active, hypophosphorylated form (PP-Rb) and an inactive form. The phosphorylation of Rb is induced by Cdk/cyclin complexes. D.) P27, a Cyclin dependent kinase inhibitor in the G1 phase, also binds to Cyclin A/Cdk2 (CYCA) and Cyclin E/Cdk2 (CYCE) dimers to form inactive trimers (CA and CE respectively, these steps occur within the Cyclin - Cyclin dependent kinase inhibitor module). Reactions are indicated by number; white number on black background denote reactions that are allosterically regulated, reactions encircled with a dotted line are dependent on ribosome activity (eps factor in model reactions), see the specific rate equation for each of the reaction steps in Appendix 1.

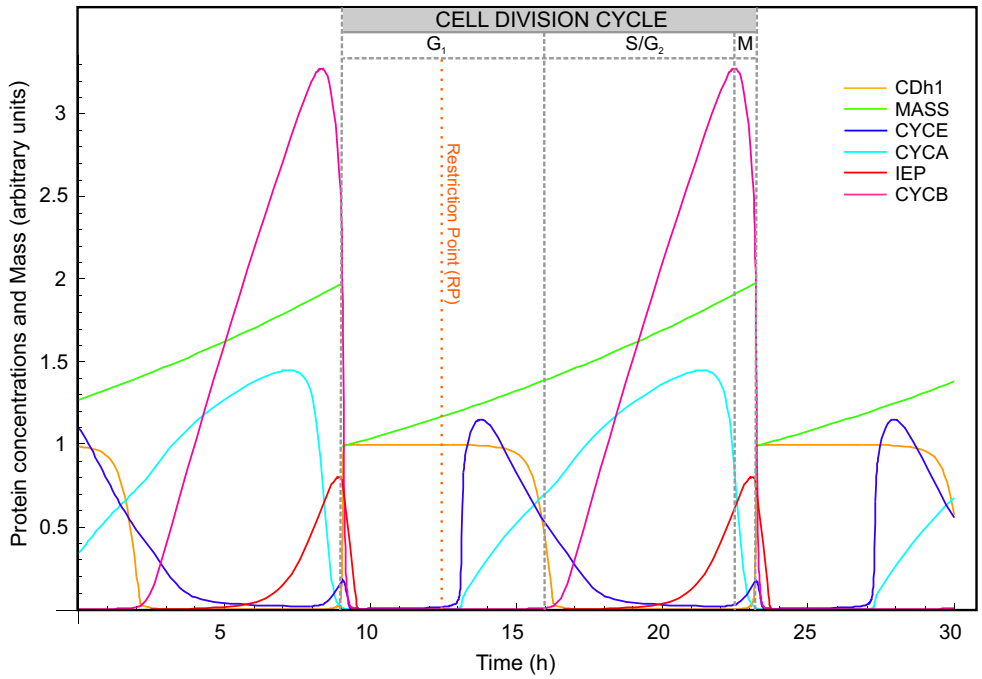

Figure 4.2: Time course of the mammalian cell division cycle. A time integration for 30 h is shown for six of the intermediates of the system. The G_1, S/G_2 and M-phases for one cell cycle are indicated in the graph. The restriction point (RP) is also depicted in the G_1-phase. It should be noted that in contrast to other switch points in the model the RP is not a hard coded event, i.e. it is not an explicit function, but rather an emergent property of the model, and it is empirically defined as the last time point where, upon cycloheximide (CHX) treatment, the cell would not finish the division cycle it started with. The CHX treatment was mimicked in the model by reducing the translation efficiency of the ribosomes (ϵ or Eps(t)), a parameter found in all synthesis steps of the model, from 1.0 to 0.5. This definition was taken from the original publication in which the model was described[56].

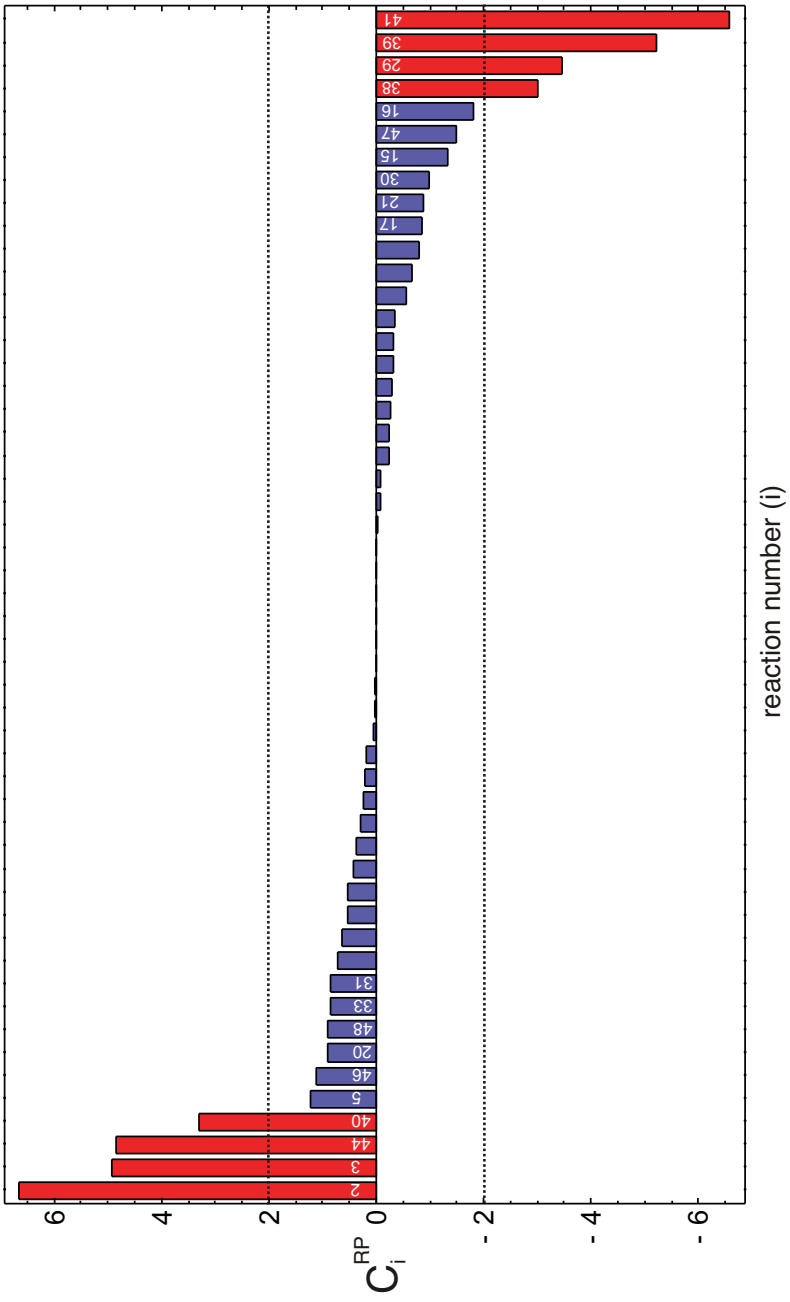

Figure 4.3: Restriction point control. The control exerted on the restriction point by the respective reaction steps (numbered as in Figure 4.1) is shown. Restriction point control is defined as the percentage change in the time point of occurrence of RP (as a fraction of total cell cycle time) upon a 1% change in activity of a reaction step. A positive control of a reaction step indicates that an increase in the activity of the step, delays the occurrence of RP.

The four steps delaying the restriction point the most (i.e. with the highest positive control values) are (i) the breakdown reaction of the delayed response genes (Reaction 2, $C_2^{RP} \sim 7$), (ii) the step involved in proteolysis of Cyclin D in the Cyclin D:p27 complex, releasing the cyclin dependent kinase inhibitor (p27), (Reaction 3, $C_3^{RP} \sim 5$), (iii) the phosphatase reaction responsible for the dephosphorylation of retinoblastoma (Reaction 44, $C_{44}^{RP} \sim 5$) and (iv) the reaction step responsible for the synthesis of p27 (Reaction 40, $C_{40}^{RP} \sim 3$).

The steps advancing the restriction point the most (i.e. with the highest negative control values) are (i) the synthesis reactions of the delayed response genes (DRGs) and Cyclin D (Reactions 41 and 39, $C_{41}^{RP} \sim -7$ and $C_{39}^{RP} \sim -5$), (ii) the cyclin mediated phosphorylation of retinoblastoma to release it from the retinoblastoma:E2F complex yielding free E2F (Reaction 29, $C_{29}^{RP} \sim -4$) and (iii) the reaction responsible for the production of Cyclin E (Reaction 38, $C_{38}^{RP} \sim -3$).

In a recent publication Yao *et al.* illustrated with a core model and experimental data of individual gene expression levels that the interplay between retinoblastoma and E2F creates a bistable switch that probably regulates the restriction point[84]. Although p27 was not modeled explicitly in this core model (its importance was stated in the text), there is still a strong similarity between the reactions that control RP, together with the feedback loops from Cyclin D and Cyclin E, in our model and the reactions involved in the bistable switch in the Yao model. Thus, according to our analysis of the model of Novak and Tyson, taken together with the summation theorem, the interplay between retinoblastoma and E2F that creates a bistable switch indeed has a strong effect on the restriction point, but with a net positive control (i.e. advancing the restriction point) which is countered by the reactions affecting p27 (i.e. delaying the restriction point).

To identify the mechanism underlying the high control coefficients of these steps for RP, we first analyzed which molecular species showed the same control pattern as was observed for the restriction point. A strong correlation between the control on RP and the concentration control coefficients of species directly involved in the molecular machinery governing the restriction point is to be expected. To test this we plotted the concentration control coefficients for

the model variables against the RP control for each of the reaction steps (Figure 4.4). For 9 of the 23 molecular species a strong correlation was observed, with some species showing a positive correlation while others have a negative correlation and that all species have a different slope in the correlation plots (note that the y-axes between the plots differ). The 9 variables that showed a strong correlation were Cyclin A, Cyclin D, Cyclin E, Cyclin E:p27 complex, p27, hyperphosphorylated retinoblastoma, E2F transcription factor, unphosphorylated retinoblastoma and unphosphorylated retinoblastoma bound to E2F transcription factor. All of these species either reside in the early and delayed response genes module, in the cyclin - cyclin dependent kinase inhibitor module or the retinoblastoma - E2F transcription factor module (see Figure 4.1 modules B, C and D). These are the same three modules that also contain the aforementioned eight steps with the highest absolute C_i^{RP} values.

A sensitivity analysis for the system variables was made at the restriction point. For this we initialized all variables in the model at their concentrations at RP, except for one variable to which we made a small perturbation. A subsequent simulation was analyzed with respect to cell cycle completion, i.e. testing whether the perturbation made to the one variable could prevent RP. The perturbation we made to the variable was to change its value to a value it had just before RP (i.e. followed its integration path back in time). In this way we determined the minimal time period that a variable must be regressed from RP along its time integration in order to stall the cell cycle progression. From this analysis it was evident that the RP was most sensitive for changes made to the Cyclin E/Cdk2:p27 complex; changing its value to the value it had 0.04 s before the RP resulted in the cells entering quiescence. The species which values needed to be regressed 0.5 s or less to prevent RP are listed in Table 4.1, each of these variables also showed a good correlation in Figure 4.4.

The six metabolites for which RP showed a high sensitivity each had a different gradient in the correlation plots (Figure 4.4); for some intermediates the correlation was positive, for others negative and each had a different slope. The correlations observed in Figure 4.4 suggest that several of the intermediates also correlate with one another (independent of which reaction is perturbed). Such

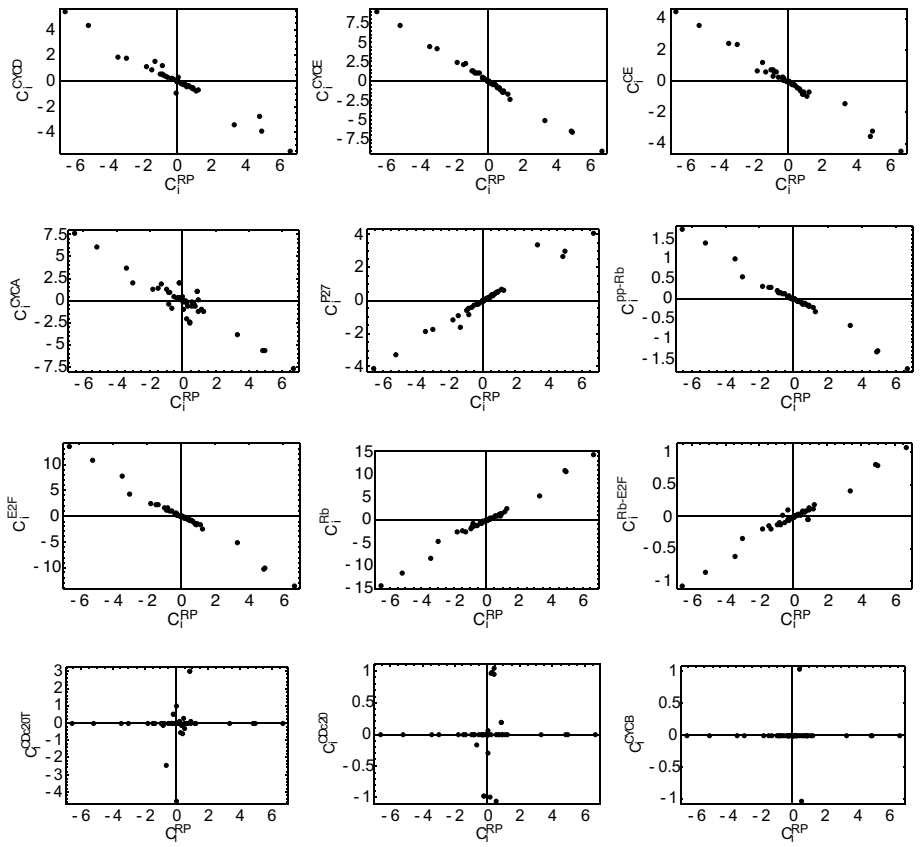

Figure 4.4: Correlation Plots for Concentration Control coefficients and RP control. Species that showed a good correlation between their concentration control coefficients and restriction point control coefficients are shown in the top nine figures. To illustrate the contrast, we also show plots for three species that did not show a good correlation in the bottom figures. Cyclin E/Cdk2:p27 is abbreviated to CE on the axis label. See text for further details.

Table 4.1: Species dependent regression time necessary for cells to enter quiescence. The six molecular intermediates for which the RP showed the highest sensitivity were each regressed in time (while initializing all other intermediates at their RP concentrations) until, upon subsequent simulation the cells enter quiescence. This minimal time that a specie must be regressed to prevent RP is listed as Regression time in the table. Also the RP concentration and the percentage change in concentration of the intermediate concentration at the regression time point compared to the RP are given. (AU=arbitrary units)

Specie	Regression time (s)	% change in concentration	Concentration at RP (AU)
CE	0.04	0.0003	0.48
CA	0.18	0.004	0.02
P27	0.22	-0.001	0.86
E2F	0.22	0.004	0.35
CYCE	0.47	0.007	0.01
Rb	0.54	-0.009	0.27

covariances between intermediates make it difficult to asses a causal relation. The RP showed the highest sensitivity for changes in the concentration of Cyclin E/Cdk2:p27 (Table 4.1); all of the other species needed to be perturbed more, either in terms of time regression or in terms of percentage change in their concentrations. This high sensitivity indicates that this intermediate is important for the regulation of RP, and we tested whether the difference in slopes in the correlation plots could be related to co-correlations between the intermediates and Cyclin E/Cdk2:p27.

For this we first determined the co-control coefficients of Cyclin E/Cdk2:p27 with the 9 intermediates that showed a good correlation in Figure 4.4. A co-control coefficient is defined as the ratio of two concentration control coefficients and quantifies the correlation between the two intermediates upon a small perturbation of a reaction step[42]. Interestingly, the values for the co-control coefficients were largely independent on the reaction step that was perturbed, i.e. two intermediates would co-vary, independent of which step was perturbed. Thus, the co-control coefficients of the model species with the Cyclin E/Cdk2:p27 com-

plex quantify the extent that these species co-vary with the complex. For example, Cyclin E/Cdk2 (CYCE) and Cyclin E/Cdk2:p27 (CE) showed a positive co-variation, with a co-control coefficient ${}^{i}O_{CE}^{CYCE}$ of 0.53, indicating that changes in the concentration of CE were correlated with roughly half the concentration change in CYCE. In contrast CE is negatively correlated with $p27^{Kip1}$, i.e. if the one goes up the other goes down, quantitatively expressed in a co-control coefficient, ${}^{i}O_{CE}^{p27}$ of -1.2.

Subsequently, we calculated the ratio of the gradients in the correlation plots (Figure 4.4) for the intermediates and for Cyclin E/Cdk2:p27. For each of the intermediates the ratio of its gradient in the correlation plot and the gradient of Cyclin E/Cdk2:p27, was close to the value of the co-control coefficient of the intermediate with Cyclin E/Cdk2:p27. For example the gradient ratio for Cyclin E/Cdk2 and Cyclin E/Cdk2:p27 equals 0.49 and for $p27^{Kip1}$ and Cyclin E/Cdk2:p27 the ratio equals -1.1 (these values are close to the respective co-control coefficients 0.53 and -1.2 as calculated above). This result is in agreement with the hypothesis that the correlations observed in Figure 4.4, between changes in system intermediate concentrations and RP, can be accounted for by co-correlations of those intermediates with Cyclin E/Cdk2:p27.

The observation that Cyclin E/Cdk2:p27 needed to be regressed for the shortest time period (Table 4.1) indicated that this molecular specie on its own could prevent RP. Regressing any of the other species further back in time could potentially effect RP indirectly via Cyclin E/Cdk2:p27. We further tested this by analyzing the effect on Cyclin E/Cdk2:p27 concentration upon perturbing each of the other variables to which the RP showed a high sensitivity. Indeed, as can be seen in Figure 4.5a, changing any of these variables to such an extent that they interfered with the RP did lead to a change in Cyclin E/Cdk2:p27. Each of the curves in Figure 4.5a is the result of a separate time simulation for the Cyclin E/Cdk2:p27 concentration upon a perturbation of the indicated (red circle) model variable. The wt curve is the reference curve where no perturbation was made. The time point (x-axis value) corresponding with the red symbols indicates RP. From the figure it can be seen that the shift brought about to the RP was in very good agreement with the extent that the concentration of Cyclin

E/Cdk2:p27 was effected by the perturbation; for most metabolite perturbations RP was shifted to the time point where the Cyclin E/Cdk2:p27 complex reached a critical concentration. Since a causal relation between Cyclin E/Cdk2:p27 concentration and the RP would necessitate that for each perturbation of the complex the RP must shift accordingly, we perturbed all reaction steps with a high control on RP and plotted the occurrence of RP together with the trajectory for Cyclin E/Cdk2:p27 (Figure 4.5b). The reactions that were perturbed for each of the curves in the figure are indicated by number (corresponding with the numbers in Figure 4.1). Again a very good correlation, in excellent agreement with the shift in RP upon metabolite perturbations was observed for the reaction perturbations. The correlation plots along with the sensitivity analysis are indicative of a causal relation between the Cyclin E/Cdk2:p27 concentration and RP; independent of the type of perturbation made, a critical Cyclin E/Cdk2:p27 concentration must be reached for RP transition.

4.3.1 RP control in Cancer Cells

Deregulation of the restriction point is implicated in almost all tumor cells and it has been suggested that regulation of the restriction point is essential to prevent cells from becoming cancerous[58]. We thus investigated whether the species shown by our analysis to alter the restriction point were indeed implicated in malignancies in mammals. Comparing phenotypic observations of tumor cells with our analysis results, we indeed observed that changes to the cells lines that would lead to an increased concentration of Cyclin E/Cdk2:p27 concentration, such as cyclin E overexpression[66,65,37,73] and $p27^{Kip1}$ downregulation[59,26,28,37,73] yielded uncontrolled tumour proliferation in a wide range of human tissues. Furthermore it was observed that in aggressive stomach, prostate, breast, lung and pituitary cancers, $p27^{Kip1}$ levels were low, either due to degradation or due to translocation to the cytoplasm[86,16]. These observations are in agreement with our co-control analysis; the co-control coefficients, ${}^{i}O_{CE}^{CYCE}$ = 0.53 and ${}^{i}O_{CE}^{p27}$ = -1.2 quantify a strong positive correlation between cyclin E and Cyclin E/Cdk2:p27 and a strong negative correlation between p27 and Cyclin E/Cdk2:p27, where these

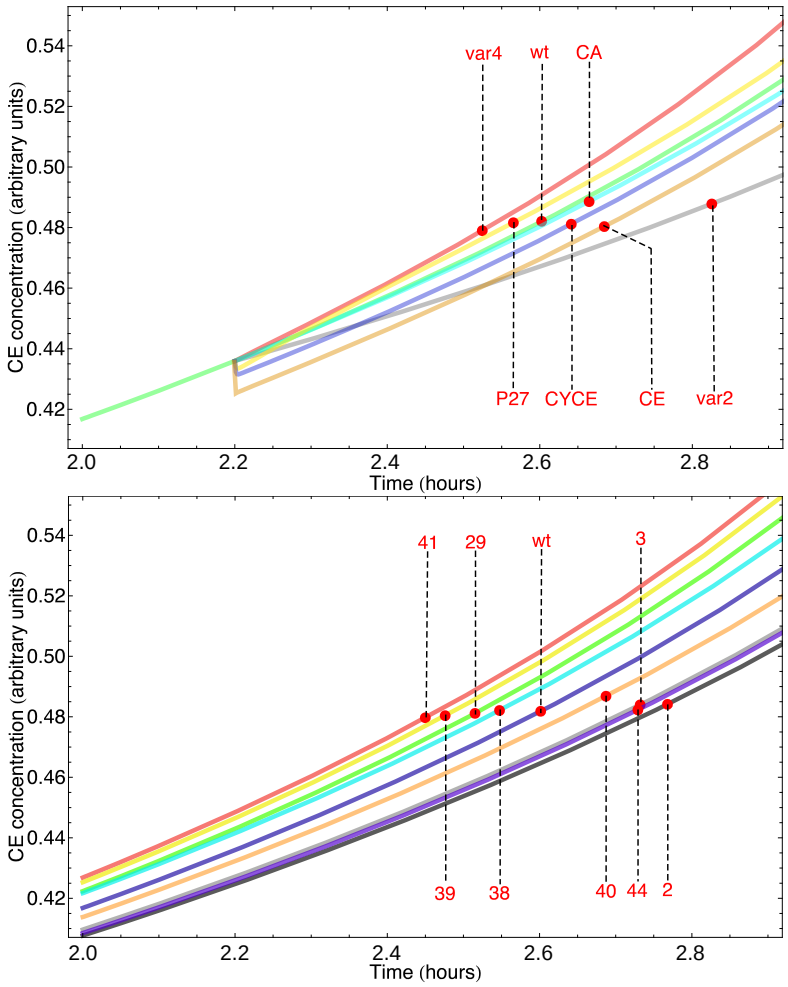

Figure 4.5: Control of the restriction point via the Cyclin E/Cdk2:p27. For each of the six species towards which RP showed a high sensitivity (see Table 4.1) a perturbation was made to its concentration such that it would affect RP, while all other variables where initialized with their RP concentrations. The results of the subsequent time integrations, following Cyclin E/Cdk2:p27 concentration and the occurrence of RP, are plotted in (a), with the points in the graphs denoting the time point of RP (x-axis) and the concentration of Cyclin E/Cdk2:p27 (y-axis). For each simulation the perturbed variable is indicated. In (b) the results of similar integrations are shown, now after perturbation of the 8 reactions that had a high RP control.

co-control coefficients are largely independent on which step is perturbed. These observations and model analyses lead us to hypothesize that RP is advanced in

cancer cell lines due to increased concentration of Cyclin E/Cdk2:p27.

4.4 Conclusions

In cancer cells restriction point control appears to be completely absent. On the basis of an extensive analysis of a detailed kinetic model, we hypothesize that such a shift of the RP to a much earlier point in the cell cycle might be caused by an increased concentration in the Cyclin E/Cdk2:p27 complex concentration. We showed that a perturbation of Cyclin E/Cdk2:p27 on its own was sufficient to shift the RP. In addition we showed that in perturbations of any of the reaction steps, the effect on RP could always be explained via a change in the Cyclin E/Cdk2:p27 concentration, leading us to propose that RP control by the reaction steps works via the Cyclin E/Cdk2:p27 complex. The method that we have used to quantify the control of a reaction step on any of the systems variables can be used to identify the reaction steps that would have the biggest effect on the Cyclin E/Cdk2:p27 concentration and therewith would shift RP most strongly. Furthermore, in principle the method provides with a tool to calculate the extent with which a reaction must be perturbed to shift RP back to its normal position. The precision of such predictions would of course be dependent on the quality of the mathematical model, but the analysis methods we propose here can be applied generically and are not model specific. The strength of these methods were illustrated for the analysis of RP control and the results clearly indicate that the control of RP runs mostly via Cyclin E/Cdk2:p27. An important implication would be that it should be possible to shift RP in cancer cells back to its normal point via perturbations of steps that effect the Cyclin E/Cdk2:p27 concentration.

4.5 Acknowledgements

RC and JLS acknowledge the National Bioinformatics Network (South Africa) for funding and support for the JWS Online project. FJB thanks the Netherlands Institute for Systems Biology and NWO for funding. AC acknowledges

support from the Italian research fund FIRB (project RBPR0523C3). BN thanks UNICELLSYS, YSBN and BBSRC for funding. HVW thanks EC-FPs BioSim, EC-MOAN, NucSys, UNICELLSYS, YSBN, ESF-FuncDyn, NWO-FALW and the BBSRC and EPSRC for support.

4.6 Appendix 1

Table 4.2: Mammalian cell cycle model[56] kinetics:

Reaction number	Rate equations
1	$v(1) = \mathrm{k16} \cdot \mathrm{ERG}(t)$
2	$v(2) = \mathrm{k18} \cdot \mathrm{DRG}(t)$
3	$v(3) = \mathrm{K10} \cdot \mathrm{CD}(t)$
4	$v(4) = \mathrm{K10} \cdot \mathrm{CYCD}(t)$
5	$v(5) = \mathrm{K25} \cdot \mathrm{P27}(t) \cdot \mathrm{CYCE}(t)$
6	$v(6) = \mathrm{K25} \cdot \mathrm{P27}(t) \cdot \mathrm{CYCA}(t)$
7	$v(7) = \mathrm{k24} \cdot \mathrm{CYCD}(t) \cdot \mathrm{P27}(t)$
8	$v(8) = \mathrm{k24r} \cdot \mathrm{CD}(t)$
9	$v(9) = \mathrm{K30} \cdot \mathrm{Cdc20}(t) \cdot \mathrm{CYCA}(t)$
10	$v(10) = \mathrm{K30} \cdot \mathrm{Cdc20}(t) \cdot \mathrm{CA}(t)$
11	$v(11) = \mathrm{K25R} \cdot \mathrm{CE}(t)$
12	$v(12) = \mathrm{K25R} \cdot \mathrm{CA}(t)$
13	$v(13) = \mathrm{V8} \cdot \mathrm{CE}(t)$
14	$v(14) = \mathrm{V8} \cdot \mathrm{CYCE}(t)$
15	$v(15) = \mathrm{V6} \cdot \mathrm{P27}(t)$
16	$v(16) = \mathrm{V6} \cdot \mathrm{CE}(t)$
17	$v(17) = \mathrm{V6} \cdot \mathrm{CD}(t)$
18	$v(18) = \mathrm{V6} \cdot \mathrm{CA}(t)$
19	$v(19) = \mathrm{V2} \cdot \mathrm{CYCB}(t)$
20	$v(20) = \frac{(\mathrm{K3a}+\mathrm{K3}\cdot\mathrm{Cdc20}(t))(1-\mathrm{Cdh1}(t))}{\mathrm{J3}-\mathrm{Cdh1}(t)+1}$
21	$v(21) = \frac{\mathrm{V4}\cdot\mathrm{Cdh1}(t)}{\mathrm{J4}+\mathrm{Cdh1}(t)}$
22	$v(22) = \mathrm{K34} \cdot \mathrm{PPX}(t)$

23	$v(23) = \frac{\text{K31}\cdot\text{CYCB}(t)(1-\text{IEP}(t))}{\text{J31}-\text{IEP}(t)+1}$
24	$v(24) = \frac{\text{K32}\cdot\text{PPX}(t)\cdot\text{IEP}(t)}{\text{J32}+\text{IEP}(t)}$
25	$v(25) = \text{K12} \cdot \text{Cdc20T}(t)$
26	$v(26) = \frac{\text{K13}\cdot\text{IEP}(t)(\text{Cdc20T}(t)-\text{Cdc20}(t))}{\text{J13}-\text{Cdc20}(t)+\text{Cdc20T}(t)}$
27	$v(27) = \frac{\text{K14}\cdot\text{Cdc20}(t)}{\text{J14}+\text{Cdc20}(t)}$
28	$v(28) = \text{K12} \cdot \text{Cdc20}(t)$
29	$v(29) = \text{E2F-Rb}(t)(\text{K20}(\text{CYCDT} \cdot \text{LD} + \text{LA} \cdot \text{CYCA}(t) + \text{LB} \cdot \text{CYCB}(t) + \text{LE} \cdot \text{CYCE}(t)))$
30	$v(30) = \text{P-E2F-Rb}(t)(\text{K20}(\text{CYCDT}\cdot\text{LD}+\text{LA}\cdot\text{CYCA}(t)+ \text{LB} \cdot \text{CYCB}(t) + \text{LE} \cdot \text{CYCE}(t)))$
31	$v(31) = \text{K27} \cdot \text{MASS}(t) \cdot \text{If}\left[\frac{\text{Rb}(t)+\text{E2F-Rb}(t)+\text{P-E2F-Rb}(t)}{\text{PP-Rb}(t)+\text{Rb}(t)+\text{E2F-Rb}(t)+\text{P-E2F-Rb}(t)} > 0.8, 0, 1\right]$
32	$v(32) = \text{K28} \cdot \text{GM}(t)$
33	$v(33) = \text{eps}(t) \cdot \text{MU} \cdot \text{GM}(t)$
34	$v(34) = \frac{\text{eps}(t)\cdot\text{k15}}{\left(\frac{\text{DRG}(t)}{\text{J15}}\right)^2+1}$
35	$v(35) = \text{eps}(t)(\text{K11a} + \text{K11} \cdot \text{CYCB}(t))$
36	$v(36) = \text{eps}(t) \cdot \text{K29} \cdot \text{E2F}(t) \cdot \text{MASS}(t)$
37	$v(37) = \text{eps}(t) \cdot \text{K33}$
38	$v(38) = \text{eps}(t)(\text{K7a} + \text{K7} \cdot \text{E2F}(t))$
39	$v(39) = \text{eps}(t) \cdot \text{K9} \cdot \text{DRG}(t)$
40	$v(40) = \text{eps}(t) \cdot \text{K5}$
41	$v(41) = \text{eps}(t) \cdot \left(\frac{\text{k17}\left(\frac{\text{DRG}(t)}{\text{J17}}\right)^2}{\left(\frac{\text{DRG}(t)}{\text{J17}}\right)^2+1} + \text{k17a} \cdot \text{ERG}(t)\right)$
42	$v(42) = \text{eps}(t) \cdot \left(\frac{\text{K1}\cdot\left(\frac{\text{CYCB}(t)}{\text{J1}}\right)^2}{\left(\frac{\text{CYCB}(t)}{\text{J1}}\right)^2+1} + \text{K1a}\right)$
43	$v(43) = \text{Rb}(t)(\text{K20}(\text{CYCDT} \cdot \text{LD} + \text{LA} \cdot \text{CYCA}(t) + \text{LB} \cdot \text{CYCB}(t) + \text{LE} \cdot \text{CYCE}(t)))$
44	$v(44) = \text{PP-Rb}(t)(\text{K19a}(\text{PP1T} - \text{PP1A}) + \text{K19} \cdot \text{PP1A})$
45	$v(45) = \text{E2F-Rb}(t) \cdot \text{K26R}$
46	$v(46) = \text{E2F}(t)(\text{K23a} + \text{K23}(\text{CYCA}(t) + \text{CYCB}(t)))$
47	$v(47) = \text{P-E2F}(t) \cdot \text{K22}$
48	$v(48) = \text{E2F}(t) \cdot \text{Rb}(t) \cdot \text{K26}$
49	$v(49) = \text{P-E2F-Rb}(t) \cdot \text{K26R}$

50	$v(50) = \text{Rb}(t) \cdot \text{P-E2F}(t) \cdot \text{K26}$
51	$v(51) = \text{P-E2F-Rb}(t) \cdot \text{K22}$
52	$v(52) = \text{E2F-Rb}(t)(\text{K23a} + \text{K23}(\text{CYCA}(t) + \text{CYCB}(t)))$

Model parameters in[56]:

k15=0.025; k16=0.025; J15=0.1; k17a=0.035; k17=1.; J17=0.3; k18=1.; K9=0.25;
K10=0.5; k24=100.; k24r=1.; K7a=0.;
K7=0.06; K8a=0.01; K8=0.2; K25=100.; K25R=1.; J8=0.1; YE=1.; YB=0.05; K29=0.005;
K30=2.; K1a=0.01; K1=0.06; J1=0.1; K2a=0.005; K2=2.; K2aa=0.1; K5=2.; K6a=1.;
K6=10.; HE=0.5; HB=1.; HA=0.5; LD=3.3; LE=5.; LB=5.; LA=3.;
K20=1.; K19a=0.; K19=2.; K21=1.; PP1T=1.; FE=25.; FB=2.; K3a=0.75; K3=14.;
J3=0.01; J4=0.01; K4=4.; GE=0.; GB=1.; GA=0.3; K33=0.005; K34=0.005; K31=0.07;
K32=0.18; J31=0.01; J32=0.01; K11a=0.; K11=0.15; K12=0.15; K13=0.5;
K14=0.25; J13=0.005; J14=0.005; K22=0.1; K23a=0.0005; K23=0.1; K26=1000.;
K26R=20.; K27=0.02; K28=0.02; MU=0.0061;

Definitions and steady state relations:

$$\text{PP1A} = \frac{\text{PP1T}}{\text{K21}\cdot(\text{FE}\cdot(\text{CYCA}(t)+\text{CYCE}(t))+\text{FB}\cdot\text{CYCB}(t))+1}$$

$$\text{V2} = \text{K2aa} \cdot \text{Cdc20}(t) + \text{K2a} \cdot (1 - \text{Cdh1}(t)) + \text{K2} \cdot \text{Cdh1}(t)$$

$$\text{V4} = \text{K4} \cdot (\text{GA} \cdot \text{CYCA}(t) + \text{GB} \cdot \text{CYCB}(t) + \text{GE} \cdot \text{CYCE}(t))$$

$$\text{V6} = \text{K6a} + \text{K6} \cdot (\text{HA} \cdot \text{CYCA}(t) + \text{HB} \cdot \text{CYCB}(t) + \text{HE} \cdot \text{CYCE}(t))$$

$$\text{V8} = \frac{(\text{YE}\cdot(\text{CYCA}(t)+\text{CYCE}(t))+\text{YB}\cdot\text{CYCB}(t))\cdot\text{K8}}{\text{CYCET}+\text{J8}} + \text{K8a}$$

$$\text{CYCET} = \text{CE}(t) + \text{CYCE}(t)$$

$$\text{CYCDT} = \text{CD}(t) + \text{CYCD}(t)$$

$$\text{CYCAT} = \text{CA}(t) + \text{CYCA}(t)$$

$$\text{P27T} = \text{CA}(t) + \text{CD}(t) + \text{CE}(t) + \text{P27}(t)$$

$$\text{EPS}(t) = 1$$

Chapter 5

Comparing G1/S Transition Control in yeast and mammalian cell models

5.1 Introduction

The eukaryotic cell cycle can be divided into four phases: G1, S, G2 and M, which are separated by clearly defined transitions, e.g. DNA replication starts at the G1/S transition and the G2/M transition is market by the condensation of chromosomes into visible structures. The transitions from the gap phases (G1/S and G2/M) are associated with so-called checkpoints, where a condition must be fulfilled for the transition to occur. We here focus on the G1/S transition, deregulation of which has been shown to be associated with many disease states, notably cancer[84,58].

Two checkpoints have been proposed to be linked to the G1/S transition: 1) a mass assessment point, referred to as START in yeast and 2) the restriction point (coined by Arthur Pardee[58]), where mammalian cells evaluate external growth factor signals (see Chapter 4). Zetterberg and Larsson showed that cells in the G1 phase, when deprived of growth factors or pulse treated with cycloheximide, either suffer an immediate and long delay, or finish the current cell division cycle, dependent on whether the perturbation was made before or after the restriction point[85]. The restriction point is an important switch

point where cells enter either the quiescent (G0) phase or proliferate, and it appears to be strongly affected in cancer cells.

In yeast, fairly strong evidence exists for a mass assessment checkpoint for the G1/S transition. A proposed mechanism via which cells sense their mass is the accumulation of a 'sizer' protein in the nucleus[83,64]. Assuming a proportionality between cell volume and the amount of a given protein, a correlation will exist between the nuclear concentration of that protein and the cell volume, if the protein is transported into the nucleus (which volume is relatively constant). In yeast, Futcher showed that Cln3 (a G1 cyclin) accumulates at a rate proportional to the cytosolic volume[79]. Thus, a mass assessment checkpoint could function via sensing the concentration of a 'sizer' protein in the nucleus. The accumulation of the nuclear concentration of the G1 cyclin above a certain threshold level makes a transition to the S phase possible[35,79]. Futcher has reported on experiments in strong agreement with this mechanism by showing that a 10% increase in nucleus size led to an almost similar increase in critical size[79].

In contrast, the experimental evidence for the existence of such a mass assessment point in mammalian cells is less convincing. Experiments from Zetterberg are indicative for the existence of another checkpoint in addition to the restriction point. He found an inverse proportionality (See Figure 5.1) between cell mass at the start of the G1 phase and the relative increase in mass, when this increase was measured over the total G1 phase, but not when measured up until the restriction point[79]. In addition, Killander and Zetterberg have shown in mouse fibroblasts, that cells with a smaller mass at the start of the cell cycle have a longer G1 phase resulting in roughly the same mass for all cells entering the S phase[50]. Even though these result may seem compelling, the existence of a mass assessment checkpoint is still a matter of debate. For instance, Conlon and Raff[17] proposed that for size homeostasis to occur in mammalian cells there need not be any mass assessment checkpoint but this has been contested by Cooper[20] and Sveiczer *et al.*[72]. This issue was again discussed in the July 2009 issue of *Science*[77,25].

Although the restriction point and mass assessment point are distinct in mechanism, it is not so easy to experimentally distinguish between these checkpoints. It is much easier to test the proposed hypotheses with respect to the checkpoints for the G1/S phase in mathematical models, as these models make it possible to make specific perturbations and analyze their effects on both cell mass and the G1/S transition point. Cell cycle models have been constructed for over 20 years; many of these model are core models, which capture particular behavior of a system in a minimal description. However,

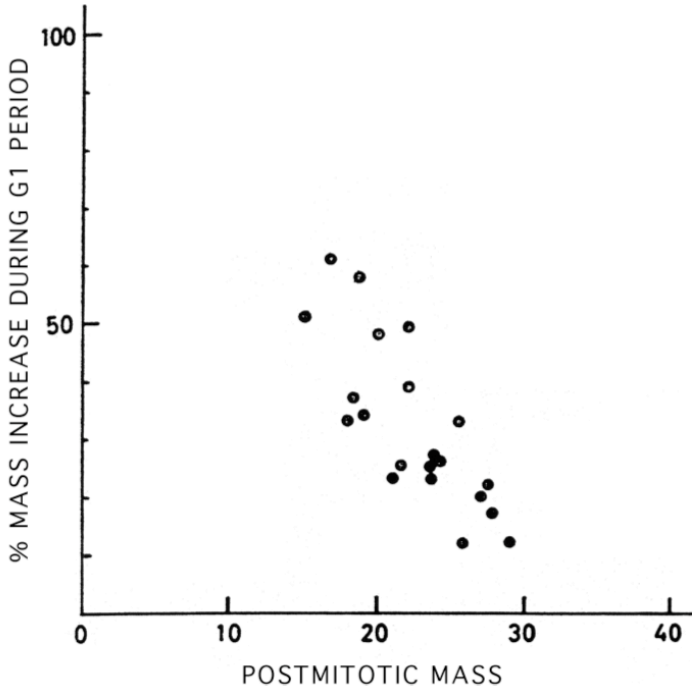

Figure 5.1: Zetterberg Experiment. Zetterberg found that cells with a small postmitotic mass have a more pronounces percentage mass increase during the G1 phase when compared with a larger mass at the beginning of the cell division cycle.

by adding more detail to these models and by fitting them to experimental data, these models have become predictive, for instance in predicting mutant behavior[14]. We have selected cell cycle models for mammalian cells and yeast and performed a comparative analysis on these models to test whether a constant mass is maintained at the G1/S transition point, irrespective of model perturbation. In this chapter we first introduce the selected models and define control on the transition point in the framework of metabolic control analysis. Then we compare the control distribution in the cell cycle models on the G1/S transition point. Subsequently we move to the control of a constant mass at the G1/S transition point and finally we discuss whether a consensus exist in these models with respect to the above described debate.

5.2 The models

Cell cycle models for budding yeast and mammalian cells, in which the Cdh1/APC complex was explicitly modeled and which contained a mass (or volume) component, were selected from the literature. These models (which included a number of core models), varied strongly in the level of detail in which the cell cycle was described, and we identified overlapping modules between the models to construct a cell cycle network that we could use to compare the models. After having standardized the names for variable species* and reactions for the respective models, we could construct a cell cycle network containing all the reactions and species that were used in the selected models (see Figure 5.2).

We have included a conversion table for acronyms of variables as used in the models (and in this chapter) to the acronyms occurring widely in the literature (Table 5.1). Note that often implicit assumptions are made in the models, for instance clb2 is the only non-complexed B type cyclin that is modeled explicitly in budding yeast. Thus, whereas 6 type B cyclins are known to exist in budding yeast, we only use clb2 as a non-complexed species (see Table 5.1 and Figure 5.2), reflecting the assumption that all other B type cyclins are complexed with their respective kinases (and listed in capitals, e.g. CLB5).

*There is no consistent use of acronyms in the literature, and different names are used for the same proteins in different organisms, making it hard to make comparisons between models and between species. The names of variable species as they occur in the original publications are tabulated in Appendix 1 (see Tables 5.2, 5.3 and 5.4 in Section 5.8).

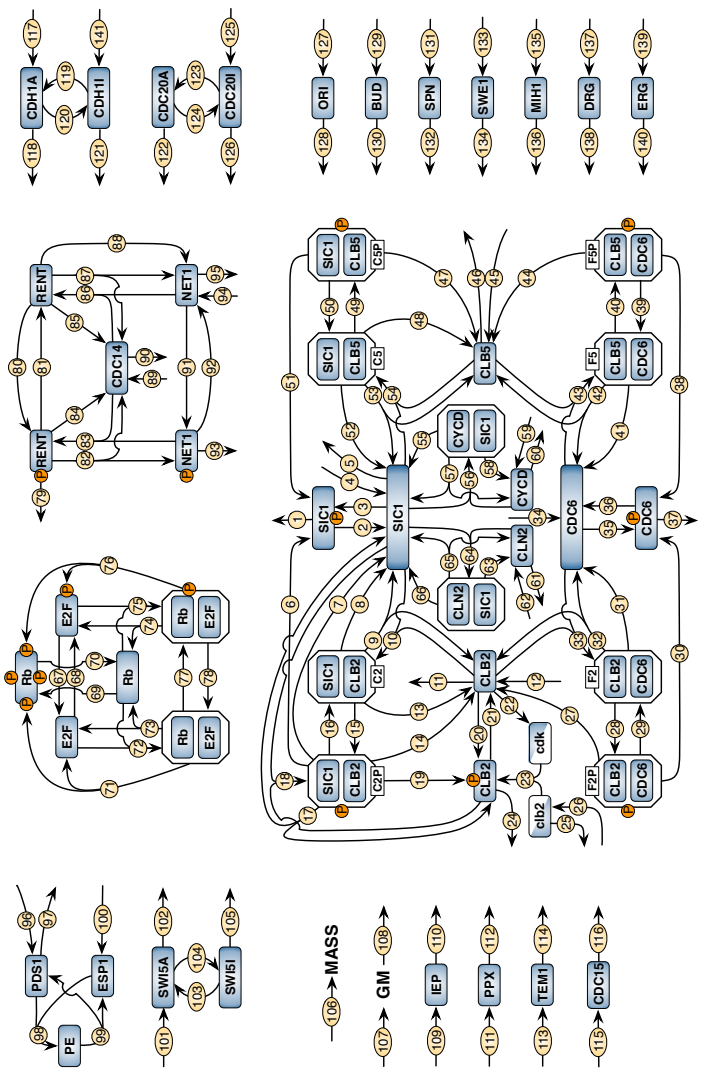

Figure 5.2: Integrated Cell Cycle Network The integration of the mathematical models of the cell cycle compared in this study yielded a network consisting of 141 reactions and 54 variable species. Each of the models analyzed can be completely represented with reactions and variable species occuring in this network.

Table 5.1: Conversion table for names of proteins and their complexes
Proteins and complexes are listed with the names used in our integrated cell cycle scheme (first column) and with the names to which they are referred to in the literature and models for budding yeast, fission yeast, mammalian cell.

	Synonym list		
Specie	**Budding Yeast**	**Fission Yeast**	**Mammalian cell**
clb2	Clb1-6	Cdc13	Cyclin B
cdk	Cdc28	Cdc2	Cdk1
CLB2	Cdc28/Clb1,2	Cdc2/Cdc13	Cdk1/CycB
CLN2	Starter Kinase (SK), Cln1,2/Cdc28	-	CycE/Cdk2
SIC1	Sic1	Rum1	$p27^{Kip1}$, Kip1
CLB5	Clb5,6/Cdc28	Cig2/Cdc2	CycA/Cdk1,2
CYCD	Cln3/Cdc28	Cdc2/Puc1	CycD/Cdk4,6
E2F	SBF, MBF, Swi4/Swi6, Mbp1/Swi6	Cdc10/Res1	E2F
CDC14	Cdc14	Clp1/Flp1	hCdc14
CDH1A	Cdh1	Ste9	Cdh1, hCdh1
CDC20A	Cdc20	Slp1	p55cdc, $p55^{cdc}$
SWE1	Swe1	Wee1	hWee1
MIH1	Mih1	Cdc25	Cdc25c

5.2.1 Budding yeast cell cycle models

Four cell cycle models were selected for the yeast *S. cerevisiae*[76,21,15,14]. All the budding yeast models contained the following species: CDC20, active CDH1A, CLB2, CLN2, SIC1 and MASS, around which we defined the modules for our comparative analysis.

The Tyson model[76] has 8 variables (proteins and their complexes) and is an extension of a core model also included in our comparative analysis. The core model illustrates the antagonistic interactions between cyclin-dependent kinases and the anaphase promoting complex that causes a cell to progress from the G1 to the S-G2-M state. This core model was extended by including a cyclin dependent kinase inhibitor and a starter kinase (see Figure 5.3), to give a simplified description of the cell division cycle in budding yeast.

The Csikasz model, (Figure 5.4) consists of 14 ordinary differential equations (ODEs) with 35 reactions and was constructed by including budding yeast

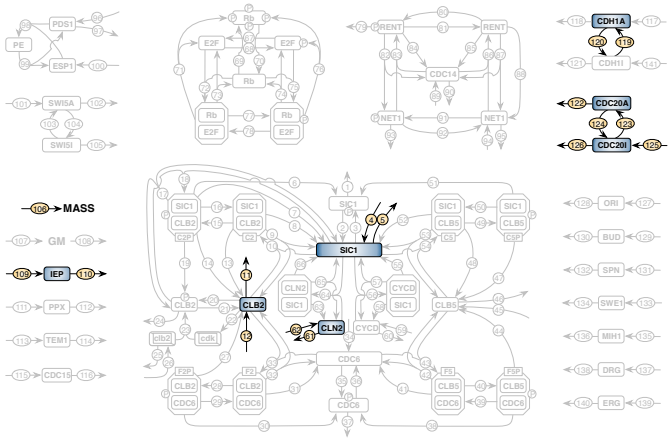

Figure 5.3: Budding yeast cell cycle model: Tyson

specific parameter values in a generic model for the eukaryotic cell cycle[21]. This generic model can be used to construct species-specific models for budding yeast, fission yeast, frog oocytes and mammalian cells by selecting, from the generic eukaryotic cell cycle model, the appropriate modules and using the unique parameter set for the specific organism.

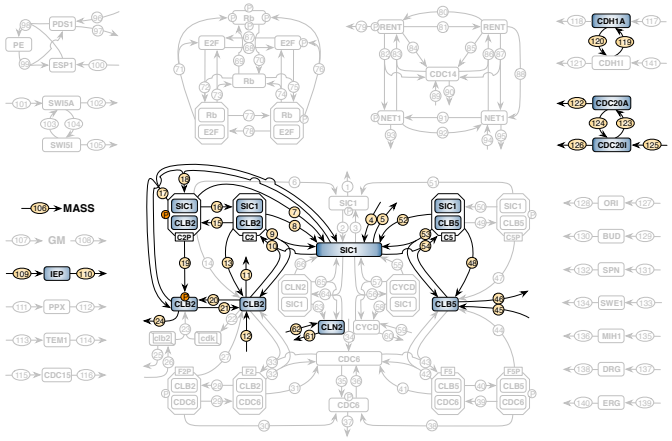

Figure 5.4: Budding yeast cell cycle model: Csikasz

Chen *et al.* constructed two kinetic models of budding yeast published four years apart. The first model (see Figure 5.5), published in 2000[15] consisting of 13 ODEs and 30 system processes, was constructed to describe the molecular events controlling "Start" and "Finish" in wild type cells and 50 mutants. As new information about the M-to-G1 transition ("exit from mitosis") of budding yeast became available, Chen *et al.* published a kinetic model of budding yeast in 2004[14] that could describe wild type cells and 120 mutants cells (of the 131 mutants known at the time). The latter model (see Figure 5.6) consists of 36 ODEs with 95 system processes and 2 events.

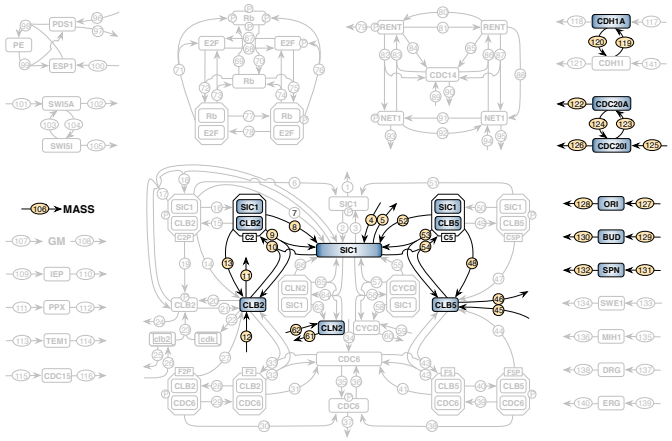

Figure 5.5: Budding yeast cell cycle model: Chen

5.2.2 Mammalian cell cycle models

Three mammalian cell cycle models were included in our comparative analysis[21,56,18]. The Csikasz2 model depicted in Figure 5.7 was constructed in a similar manner as the budding yeast cell cycle model from the same publication[21], but now mammalian cell cycle modules and specie-specific parameters were included in the generic eukaryotic cell cycle model. The model consists of 12 ODEs with 29 system processes and one event.

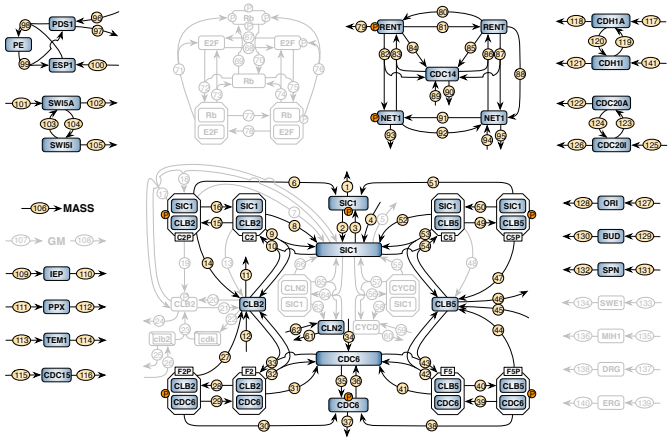

Figure 5.6: Budding yeast cell cycle model: Chen2

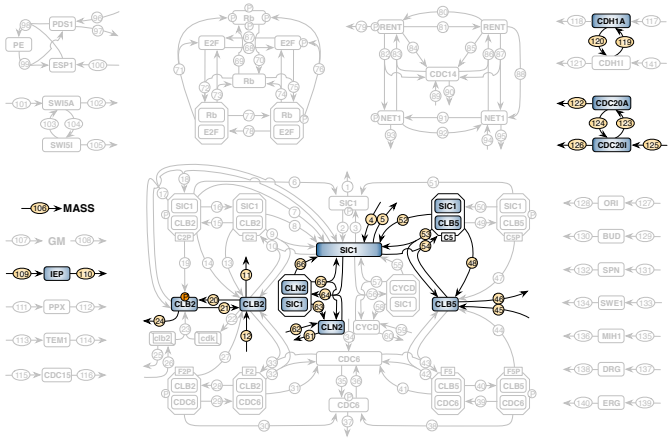

Figure 5.7: Mammalian cell cycle model: Csikasz2

The Novak model was constructed on the basis of a budding yeast model to which auxiliary processes found in mammalian cells, such as a module describing the interaction of retinoblastoma protein and E2F transcription factor as well as a growth factor sensing module were added[56]. The model consists of a system of 18 ODEs with 40 system processes and 1 event (Figure 5.8). The Conradie

model (Figure 5.9) consists of 23 ODEs with 50 reactions and was constructed on the basis of the Novak model. The algebraic equations in the original model, used for the description of the regulatory mechanism of phosphorylation of the retinoblastoma protein (Rb) and its inhibitory effect on the E2F transcriptional activation protein, were converted into ODEs (see Chapter 4).

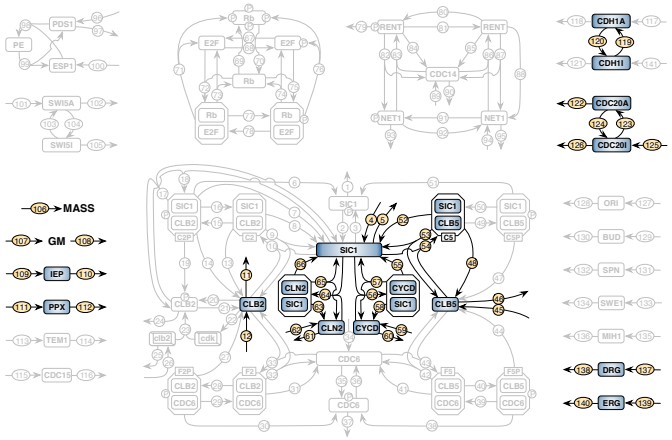

Figure 5.8: Mammalian cell cycle model: Novak

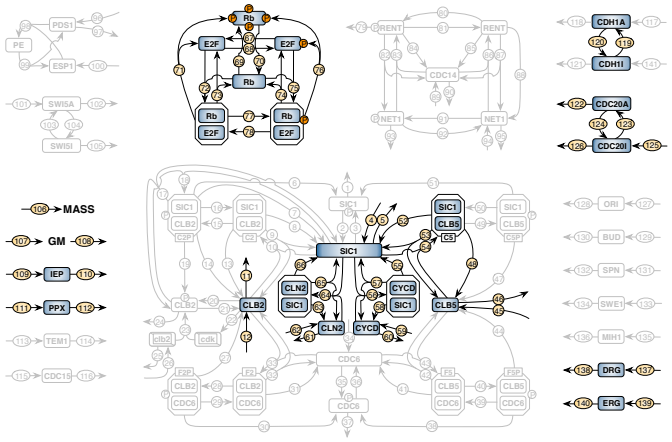

Figure 5.9: Mammalian cell cycle model: Conradie

5.2.3 Core cell cycle models

Three core models were included in our comparative analysis,[69,71,76]. Two of these models were very different from the other models in our study and the third one was a core model from the Tyson group.

The Srividhya model[69] is a general eukaryotic cell cycle model, consisting of 7 ODEs and 13 processes, with a delay equation for the description of the activation of the APC by clb2, acting as a spindle checkpoint.

The Surovstev model[71] is build within a whole cell modeling framework. The cell cycle part of the model consisted of 5 ODEs and 13 processes. The model is build from a physico-chemical perspective with the cytosolic volume and the membrane surface modeled explicitly.

In the Tyson2 model[76], focus is placed on the antagonistic interaction between the cyclin dependent kinases and the APC. The model consists of 6 ODEs and 12 processes.

5.3 Definition and position of the G1/S transition point

The G1/S transition point is defined by the start of DNA synthesis, which coincides with the increase in the concentration of Cyclins/Cdk and a decrease in the CDH1 concentration. For our analyses we have used the point where the CDH1 concentration has dropped halfway from its maximum value (in the G1 phase) to its minimum value (in the S phase) to quantify the time point where the G1/S transition occurs.

For the non core models the G1/S transition point occurred at positions in the cell division cycle, varying between approximately 30% and 70% of the complete cell cycle (Figure 5.10). All of the models showed a switch type behavior where the CDH1 concentration drops rapidly from its maximal to its minimal value.

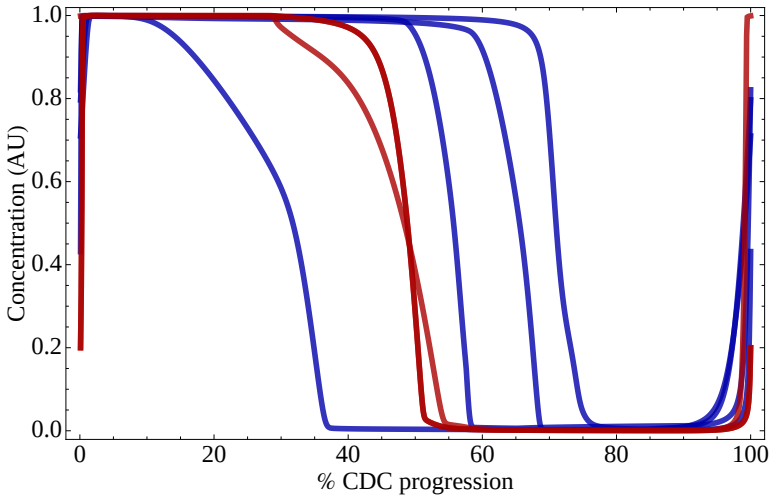

Figure 5.10: Cdh1 concentration for budding yeast (blue) and mammalian cell (red) models as the cell progresses through one division cycle. The Novak and Conradie models followed the same trajectory.

After defining the G1/S transition point, and noting that the location of the point differs markedly between the different models we analyzed which of the

reactions in the models were important for the positioning of the transition point using metabolic control analysis.

5.4 Control of the G1/S transition

To compare a set of models we identified the proteins and their complexes that were represented in all the models within the set. Subsequently, for each of these common species we grouped the reactions that either formed or degraded that specie in a module. These modules give the structural basis on which we compared the models. For instance in all the budding yeast models CLB2 was represented; in the simplest model there were only 2 reactions that synthesized/degraded CLB2, while in the most detailed budding yeast model there were 8 reactions in that module. When we compare control distributions in the different models, we compare the control of these modules. This modular approach makes it possible to compare models that differ greatly in detail. We first determined the control of the reactions modules on the position of the G1/S transition.

5.4.1 G1/S transition control in budding yeast

As a first analysis we compared several budding yeast cell cycle models to determine how the respective cell cycle reactions control the G1/S transition. As explained in Section 5.4, we first defined the modules occurring in all budding yeast models: these were the reactions producing and consuming active Cdc20A, inactive Cdc20, active Cdh1, CLB2, CLN2 and SIC1 as well as the step describing MASS accumulation. Subsequently we determined the control of each of the reactions by making small perturbations and analyzing its effect on the position of the G1/S transition point. For more details on this method see Section 2.3. The control of the reactions in each of the modules were added together, giving the overall control exerted by this module on the positioning of the G1/S transition point (where the transition point is expressed as the length of the G1 phase

divided by the total length of the cell cycle). In Figure 5.11, we have shown the control of the seven modules on the G1 fraction of the cell cycle, for the four budding yeast models.

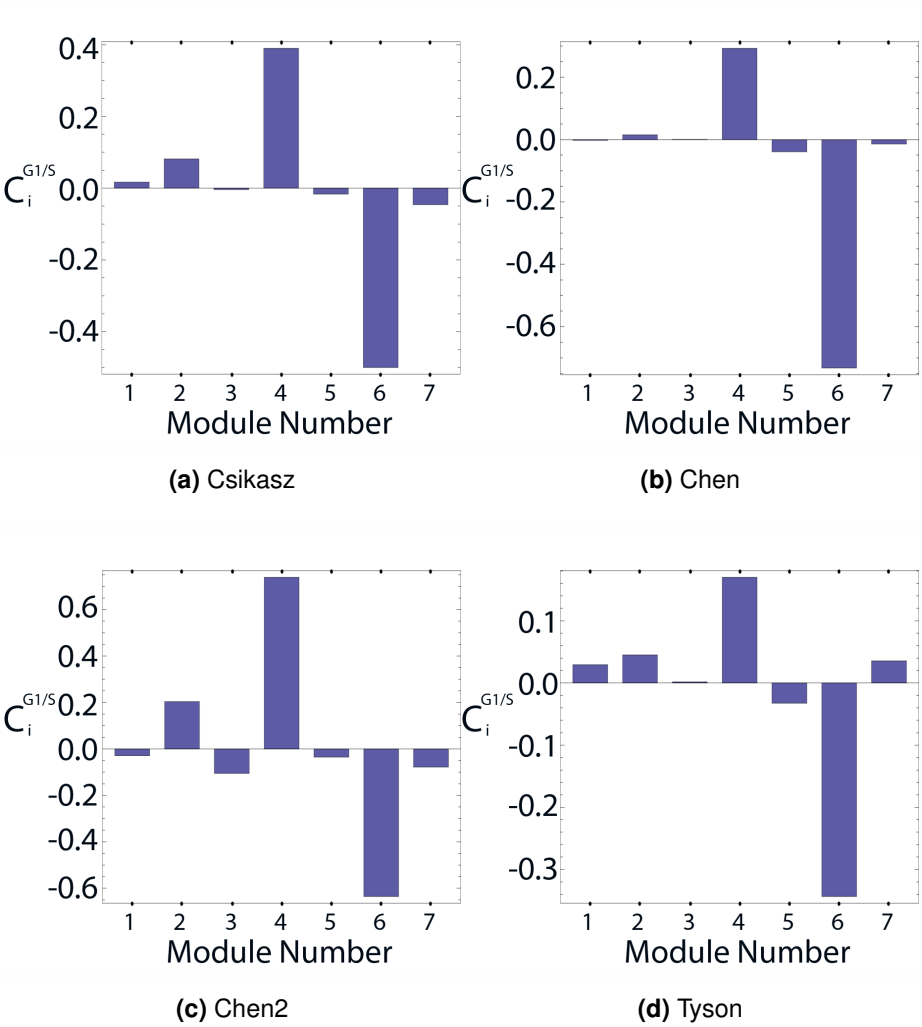

(a) Csikasz **(b)** Chen

(c) Chen2 **(d)** Tyson

Figure 5.11: Control on the length of the G1 phase as a fraction of the cell cycle for the budding yeast models The control on the G1 phase fraction by the modules of the following variable species: Cdc20A (1), Cdc20I (2), Cdh1A (3), CLB2 (4), CLN2 (5), MASS (6), SIC1 (7), is shown for the four budding yeast cell cycle models.

The control distribution over the seven modules is strikingly similar, with

the majority of the control residing in two of the modules, the MASS and CLB2 modules, with most of the other modules having only a small contribution to the positioning of the G1/S transition point. A positive control (leading to an increasing in the length of the G1 phase relative to the total cell cycle length) was exerted by the Cdc20I, and CLB2 modules in all models, whereas the CLN2, and MASS modules had a negative control on the relative G1 phase length.

The control coefficients are not just a quantification of the sensitivity of the system for perturbations in reaction rates. As derived in Section 2.3, summation theorems exist for the control coefficients of a system, and for the G1/S transition point (expressed as the fractional length of the G1 phase to the total length) the theorem states that the control coefficients should sum up to 0. Thus, by definition control on the G1/S transition point must be distributed over the system, resulting in no net change in the transition point if al reactions were to be perturbed simultaneously (with the same percentage change). Although our comparative analysis does not necessarily include all reactions of the system (we focussed on the reactions producing or degrading the common intermediates), we made sure that our modules included the vast majority of the controlling reactions.

5.4.2 G1/S transition control in mammalian cells

Analogous to the definition of modules for the budding yeast models we defined modules for the mammalian cell cycle models, grouping the reactions synthesizing or degrading the following common species: CA, Cdc20A, Cdc20I, Cdh1, CLB2, CLB5, CLN2, CE, IEP, MASS, and SIC1. In Figure 5.12, we have shown the control of the eleven modules on the G1 fraction of the cell cycle, for the four budding yeast models.

Also for the mammalian models a strikingly similar distribution for G1/S transition point control was observed for the different models. As was found for the budding yeast models, in the mammalian cell cycle models, the MASS and CLB2 modules have the highest control on the G1/S transition. Positive control in all three models was observed for the Cdc20A, Cdc20I, CLB2, IEP, and SIC1 modules, while the CLB5, CLN2, CE and MASS modules had a negative control

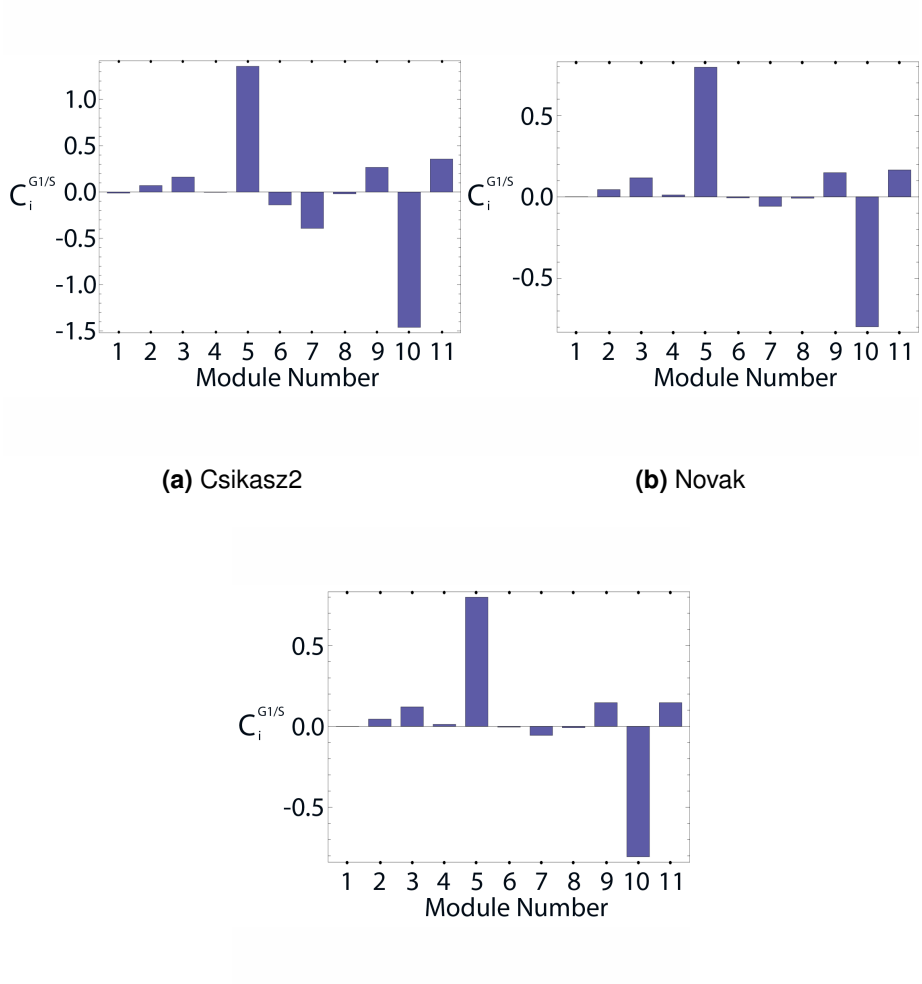

(a) Csikasz2 **(b)** Novak

(c) Conradie

Figure 5.12: Control on the length of the G1 phase as a fraction of the cell cycle for the mammalian models The control on the G1 phase fraction by the modules of the following variable species: CA (1), Cdc20A (2), Cdc20I (3), Cdh1 (4), CLB2 (5), CLB5 (6), CLN2 (7), CE (8), IEP (9), MASS (10), SIC1 (11), is shown for the three mammalian cell cycle models.

on the G1/S transition point.

The distribution of control over the different modules was very similar, not only within the two groups of models, but also between the two groups, where the most striking result was the high positive control for the CLB2 module and the strong negative control for the MASS module. To test whether we could

pin-point these distributions to a particular mechanism we analyzed several core models, differing strongly from the detailed models.

5.4.3 G1/S transition control in core models

For the core models we chose the Srividhya model[69], the Surovstev model[71] and the Tyson2 model, a general cell cycle model by Tyson *et al.*[76]. For a brief description of the models see Section 5.2.3. We defined three modules for the core models, these include the reactions synthesizing/degrading the CDH1A, CLB2 and MASS species. Note that in these core models some of the reactions occur in more than one module.

In Figure 5.13 we show the G1/S transition control distribution over the modules for the three models. For the core models a positive control by the MASS module was obtained, which implies that an increase in the MASS accumulation or growth rate would lead to an increase in the percentage of time that a cell would reside in the G1 phase. This is a very different control structure from that obtained with the more realistic models.

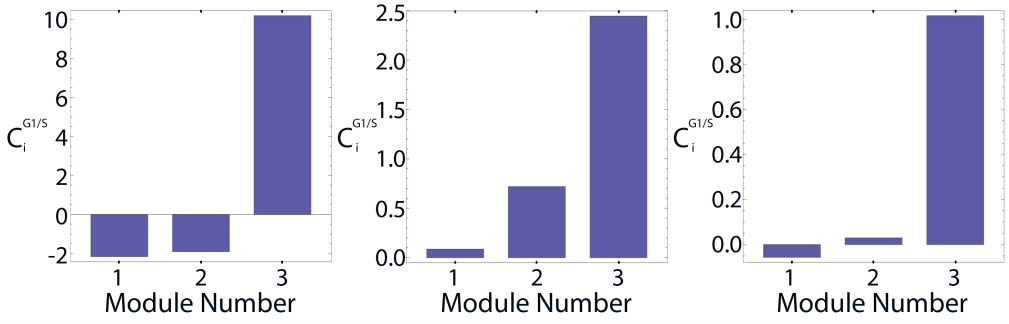

(a) Srividhya **(b)** Surovstev **(c)** Tyson2

Figure 5.13: Control on the length of the G1 phase as a fraction of the cell cycle for the core models The control on the G1 phase fraction by the modules of the following variable species: CDH1A (1), CLB2 (2), MASS (3), is shown for the three core cell cycle models.

Tyson[76] has illustrated how certain yeast like behavior could be obtained by adding a starter kinase and a cyclin dependent kinase inhibitor in a core model. We added these two reaction steps successively to a core model (Tyson2) and analyzed the resulting models (respectively Tyson3, core model with starter kinase, and Tyson, core model with both reactions added, equal to the model treated in the detailed budding yeast models).

The simple addition of a single reaction, the starter kinase, changed the control structure that the reaction modules in the core model (Tyson2), exerts on the time of G1/S transition point to that of the more detailed cell cycle models (Figure 5.14a vs. Figure 5.14b). The further addition of a cyclin dependent kinase inhibitor (CKI) did not markedly change the control exerted by the reaction modules on the time of the G1/S transition point (Figure 5.14c vs. Figure 5.14b).

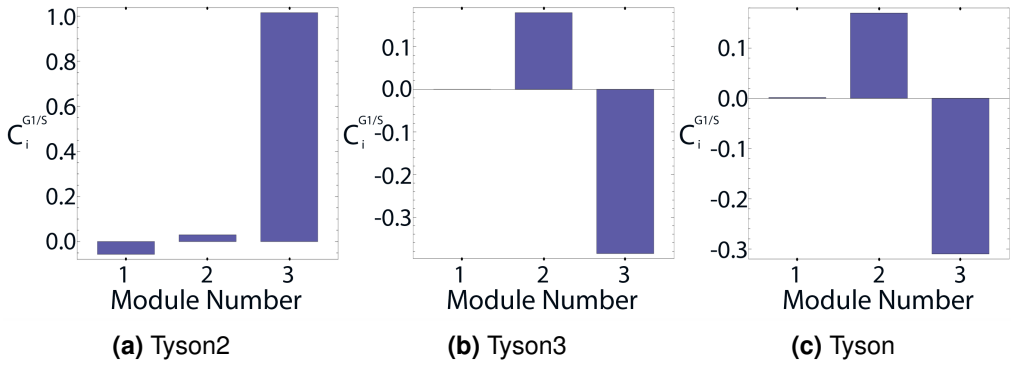

(a) Tyson2 **(b)** Tyson3 **(c)** Tyson

Figure 5.14: Comparison of cell cycle control in three tyson core models. The control on the G1 phase fraction by the modules of the following variable species: CDH1A (1), CLB2 (2), MASS (3), is shown for the three Tyson cell cycle models.

Thus far we have defined the G1/S transition point and determined the control on the positioning of the transition point in the total cell cycle. We now move to the control of mass (cell size) at this transition point. First assessing the robustness of constant cell mass at the transition point towards perturbation of the reaction rates in the system.

5.5 Control of mass at the G1/S transition point

A control coefficient quantifies the percentage change in a systems property (such as the cell mass at the G1/S transition point) upon a 1 percent change in a reaction rate. A such, it quantifies the robustness of the systems property for changes in reaction rate perturbations; the smaller the control coefficient, the larger the robustness of the property. Hans V. Westerhoff (personal communication) have used this characteristic of control coefficients to define the robustness for systemic properties as $R = 1/C$. We have determined the control coefficients of each reaction step on the size at the beginning of the cell division cycle and at the G1/S transition. For each of the models, we calculated the average control of all the reactions in a model on both the cell size at the beginning of the G1 phase and at the end of the G1 phase (Figure 5.15).

Figure 5.15 shows that the core models display a high average control coefficient value[†] on the size of cells at the G1/S transition point (average value±standard deviation; Srividhya 2.6±5.4; Tyson2, 1.5±1.5; Surovstev 0.7±0.5) as well as on the size of cells at the beginning of the cell division cycle. For the mammalian cell cycle model intermediate values for the control coefficients were obtained (average value/standard deviation; Novak 1.3±1.5; Conradie 1.17±1.33; Csikasz2 0.16±0.21), while the budding yeast models had the lowest control coefficients (average value/standard deviation; Chen 2 0.05±0.1; Chen 0.02±0.03; Tyson 0.02±0.02; Csikasz 0.01±0.03). Furthermore, three of the detailed yeast models (Csikasz, Chen and Tyson), not only showed a very high robustness for mass at the G1/S transition point, which was much higher than the robustness observed in any of the other models, but it was also higher than the robustness on the mass at the beginning of the G1 phase. Thus, these latter models appear to have a mechanism that corrects changes in cell size during the G1 phase; a perturbation leading to an altered cell size at the beginning of the G1 phase, leads to a much smaller change in cell size at the G1/S transition point.

Novak and Tyson[76] have shown how a core model of the cell cycle can be

[†]The average control coefficient is calculated from the absolute values of the control coefficients

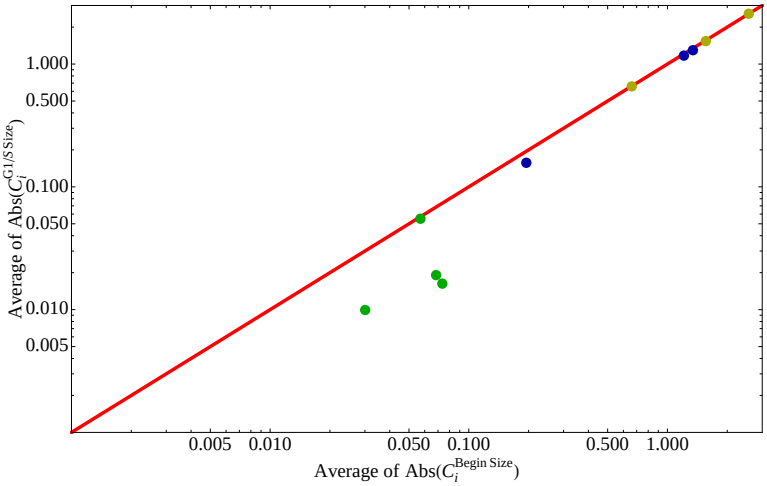

Figure 5.15: Control of cell size at the beginning and at the end of the G1 phase The average of the absolute value of the control coefficients for cell size at the beginning of a cell division cycle is plotted against the average of the absolute value of the control coefficients for cell size at the G1/S transition point. Values for the budding yeast cell models (green dots), mammalian cell cycle models (blue dots) and the three core models (yellow dots) are shown. The y=x line is indicated to make the comparison of control on cell size between the beginning and end of G1 phase easier.

converted into a simple yeast cell cycle model by the addition of two reaction steps: a starter kinase and a cyclin dependent kinase inhibitor. We have analyzed the effects of the two additions on the average of the absolute value of control coefficients for cell size at the beginning and at the end of the G1 phase (Figure 5.16). The addition of the starter kinase to the core model makes the model more stable with respect to cell size at both the beginning of the cell division cycle and at the G1/S transition point (i.e. the model makes a shift to lower average control on cell size at both time points). With the further addition of a cyclin dependent kinase to the model, an increase in the average control on size at the beginning of the cell division cycle is observed, together with a decrease in the average control on the G1/S transition point - indicative of a mass “correction” mechanism in the G1 phase.

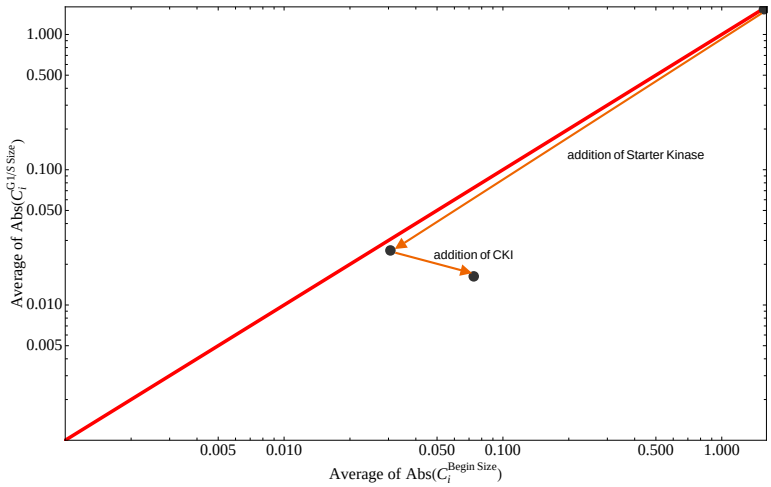

Figure 5.16: Control of cell size at the beginning and at the end of the G1 phase for core Tyson models The average control coefficient for cell size at the beginning of a cell division cycle is plotted against the average control coefficient value for cell size at the G1/S transition point. Values are shown for the core model (Tyson2)[76], the core model with the addition of a starter kinase (Tyson3), and the model with a subsequent addition of CKI (Tyson).

5.6 Discussion and conclusions

In this chapter we focussed on control of the G1/S transition, paying special attention to the robustness of cell size at the transition point for perturbation in reaction rates. We used the generally applied definition for the G1/S transition; a sharp decrease in Cdh1 and increase in cyclins/cdk complexes, to analyze a series of mathematical models for the mammalian and budding yeast cell cycle. For the analysis we used MCA to quantify the control of each of the reaction steps in the model on the length of the G1 phase (expressed as a fraction of the total cell cycle length). We subsequently defined modules of reactions around the common species in the models, and control by these modules could be used in a comparative analysis between the models. We linked the control on the positioning of the G1/S transition point to control on mass at the G1/S transition point to study the robustness of cell size at the end of the G1 phase.

A striking similarity was observed with respect to the control distribution

for the detailed kinetic models, with a strong positive control by the Cyclin B module and a negative control by the mass module. The underlying mechanisms for the similarity for the control distribution could be related to the role of a starter kinase, addition of which to a core model swapped the control of the mass module from a positive control (as was typically observed in the core cell cycle models) to a negative control (as observed in all detailed models). The control by the mass module should be interpreted as a feedback loop; the extent in which a perturbation of the mass module changes the mass, can be diminished if the change in mass has an inverse effect on the length of the G1 phase (i.e. increase in mass should lead to a decrease in length of G1 phase).

In a more direct analysis of the control of cell mass at the G1/S transition point we observed an increase in the robustness (i.e. tendency of the cell mass at the end of the G1 phase to be insensitive for perturbations) going from core models to detailed models for mammalian cells to detailed models of budding yeast cell cycle models. However, for the core models and the mammalian models this increased robustness was accompanied by an increased robustness in cell mass at the beginning of the G1 phase, not pointing at a G1 phase specific mass correction mechanism. Only for the detailed budding yeast we observed a stronger robustness for mass at the end of the G1 phase than robustness for mass at the beginning of the G1 phase. Such a mass correction mechanism in the G1 phase for budding yeast appears to be in strong agreement with the role that has been attributed to the G1/S phase checkpoint in this organism.

To find the molecular basis for this correction mechanism would improve our understanding of the mass assessment checkpoint, but the current models do not contain sufficient molecular detail for such an analysis. This points to the relativity of detail in the "detailed" kinetic models that we have analyzed. Compared to the detail in which molecular interaction maps are described for the cell cycles (see Figure 2.2)[51], our current quantitative understanding of these interactions is very limited, often we only have semi-quantitative information (i.e. interaction is stimulatory or inhibitory), which precludes building ODE type models at such a high level of detail. Thus, even in the models that we have referred to as detailed, many of the reaction steps are combinations of a number

of reactions. This does not invalidate the use of such models or the relevance of analysis results for such models. For instance, by casting our analysis in the modular MCA framework [12,11,43,81] it is possible to relate control within a module to the individual reactions in the module, if the module were to be opened up at a later stage.

We first look at the molecular detail for the G1/S transition in the models that we have analyzed and then discuss some of the more detailed models that have been constructed specifically for this transition. At the heart of the G1/S transition lies the bistability between Cdh1/APC and CycB/Cdk complexes brought about by their antagonistic interaction: CycB/Cdk inactivates Cdh1 and Cdh1/APC attaches a destruction label to CycB/Cdk to induce proteolysis [76]. In addition to this direct "negative" effect of CycB/Cdk on Cdh1/APC, the complex also has a delayed "positive" effect via the activation of Cdc20 which in its turn stimulates the synthesis of Cdh1. The effect of growth on this bistability is incorporated in the core tyson model (Tyson2) by adding a mass term to the rate equations for the reactions that are affected by CycB/Cdk. This is under the assumption that CycB concentration in the nucleus (where CycB is active and which concentration is not modeled explicit in the model) increases as cell mass increase. This assumption is justified by experiments in which it was shown that Cln3p, a yeast G1 cyclin accumulates at a rate that is determined by the cytosolic volume [79,35]. As the cytosol increases in size, more Cln3p accumulates, but the size of the nucleus stays relatively constant, leading to a higher nuclear Cln3p concentration.

In the core models, the effect of a growth rate increase will result in either a delay or advance of the bistable switch between Cdh1/APC and CycB/Cdk, depending on whether the "positive" or the "negative" effect of the CycB/Cdk loop is stronger. From the control analysis results on the G1/S transition of the Tyson2 core model, it can be seen that an increase in growth rate leads to a delay in the G1/S transition (mass module has a positive control on G1 phase length (see Figure 5.13c). This shows that the "positive" effect of CycB/Cdk is stronger than it "negative" effect. When the Tyson2 core model is extended to include a starter kinase (Cln2) this changes the positive control by the mass

module into a negative control. The starter kinase is an activator of the Cdh1 inactivation rate and lowering of the Cdh1 levels apparently makes the bistable switch more sensitive to the direct "negative" effect of CycB/Cdk, leading to the G1/S transition point to be advanced (i.e. take place earlier). When considering the rate equations for the starter kinase (Cln2) in both the budding yeast and mammalian cell models, it should be noted that models that appear more robust toward perturbations of cell mass at the beginning of the cell division cycle all contain a mass multiplication term in the synthesis reaction of the starter kinase. This inclusion of this mass multiplication term to the starter kinase synthesis reaction did, however, not necessarily lead to a correction mechanism in the G1 phase.

Mathematical models with more molecular detail have been published for the G1/S transition[7]. In this model a critical cell mass (Ps) has to be reached in order for the cells to start DNA replication. Furthermore the authors show that the G1/S transition point is an emergent property arising from the detailed interactions of the entire G1 to S network described in their model and that Ps is determined by parameters such as binding affinity of individual cell cycle proteins, which affect Ps independently from growth rate. Barberis *et al.* add several novel features to their model to describe the G1 to S network in detail[6,7]. These features include modeling of cell volume along with the explicit modeling of nucleus and cytoplasm volume. With these additions the new model describes cytoplasmic synthesis of proteins, starting from mRNA migration from the nucleus. Several other studies (such as Haberichter *et al.*[33], Tashima *et al.*[74] and Yao *et al.*[84]) include additional G1 phase machinery in quantitative models. However, these models describe the machinery active during the G1 phase (focussing on the restriction point) and they can not be used to study the G1/S transition point.

This brings us back to the selection of models that we have included in our comparative analysis. One could ask the question: Why did we not include all the newest models with more molecular detail on specific aspects of the cell cycle? The reason is simple; we compared the models with respect to the control of the G1/S transition phase with a specific focus on robustness of cell size at this transition. As such we were limited to cell cycle models that modeled the

complete cell cycle (necessary for us to determine the fractional length of the G1 phase to the total cell cycle length), and included the Cdh1 complex (used to define the G1/S transition point), and mass (to check for the robustness of cell size). We further limited ourselves to models for budding yeast and mammalian cells, to compare robustness of mass at the G1/S phase transition for a system where such a mass conservation has been proposed (yeast) to a system where the existence of a mass-assessment checkpoint is debated.

In a concluding remark we wish to come back to the debate with which we started this chapter: "Is there a mass-assessment checkpoint in the G1 phase of mammalian cell lines?" On the basis of our comparative analysis of mathematical models for the eukaryotic cell cycle, we could not find indications for such a mass-assessment point in mammalian cells. Although the mass at the G1/S restriction point was relatively robust to perturbations of the reactions in the network, this robustness did not come from a regulatory mechanism in the G1 phase, but was already present at the beginning of the G1 phase. This in contrast to the budding yeast cell cycle, for which we observed a much stronger robustness at the G1/S transition point compared to that at the beginning of the G1 phase, suggesting that a mass-correction mechanism is in place in the G1 phase in these cells.

5.7 Acknowledgements

RC, JLS and the JWS Online project are funded by the National Bioinformatics Network (NBN) of South Africa. RC and JLS thank Kora Holm for drawing cell cycle schemes for this manuscript and for JWS Online.

5.8 Appendix 1

Table 5.2: Species occuring in the budding yeast cell cycle models. The species as they occur in the Integrated cell cycle network are listed below, along with the specie names as they occur in the original manuscripts where the Csikasz, Chen, Chen2 and Tyson models were described. The budding yeast models could all be constructed with 38 of the 54 variable species from the integrated cell cycle network. Species that occured in all models (highlighted in bold) were used to compare the respective models.

	Budding Yeast Models			
Specie	**Csikasz**	**Chen**	**Chen2**	**Tyson**
BUD	-	BUD	BUD	-
C2 (CLB2/SIC1)	CycB - actCycB - preMPF	Clb2/Sic1	C2	-
C2p (CLB2/SIC1p)	preMPF - CycB + actCycB + TriB	-	C2P	-
C5 (CLB5/SIC1)	CycA - actCycA	Clb5/Sic1	C5	-
C5p (CLB5/SIC1p)	-	-	C5P	-
CDC14	Cdc20A	-	Cdc14	-
CDC15	-	-	Cdc15	-
CDC20A	**Cdc20A**	**Cdc20**	**Cdc20A**	**Cdc20A**
CDC20I	**Cdc20T - Cdc20A**	**Cdc20T - Cdc20**	**Cdc20T - Cdc20A**	**Cdc20T - Cdc20A**
CDC6	-	-	Cdc6	-
CDC6p	-	-	Cdc6P	-
CDH1A	**Cdh1**	**Hct1**	**Cdh1**	**Cdh1**
CDH1I	-	-	Cdh1T - Cdh1	-
CLB2 (clb2/cdk)	**actCycB**	**Clb2T - Clb2/Sic1**	**Clb2**	**CycB**
CLB2p	CycB - actCycB - TriB	-	-	-
CLB5	actCycA	Clb5T - Clb5/Sic1	Clb5	-
CLN2	**actCycE**	**Cln2**	**Cln2**	**SK**
ESP1	-	-	Esp1	-
F2 (CLB2/CDC6)	-	-	F2	-
F2p (CLB2/CDC6p)	-	-	F2P	-
F5 (CLB5/CDC6)	-	-	F5	-
F5p (CLB5/CDC6p)	-	-	F5P	-
IEP	APCP	-	APC-P	IE
MASS	**mass**	**mass**	**mass**	**M**
NET1	-	-	Net1	-
NET1p	-	-	Net1T - Net1 - Cdc14T + Cdc14	-

Continued on Next Page...

Specie	**Csikasz**	**Chen**	**Chen2**	**Tyson**
ORI	-	ORI	ORI	-
PDS1	-	-	Pds1	-
PE	-	-	Esp1T - Esp1	-
PPX	-	-	PPX	-
RENT	-	-	RENT	-
RENTp	-	-	Cdc14T - RENT - Cdc14	
SIC1	**CKI - TriB - CycA + actCycA**	**Sic1T - Clb2/Sic1 - Clb5/Sic1**	**Sic1**	**CKI**
SIC1p	-	-	Sic1P	-
SPN	-	SPN	SPN	-
SWI5A	-	-	Swi5	-
SWI5I	-	-	Swi5T - Swi5	-
TEM1	-	-	Tem1	-

Table 5.3: Species occuring in the mammalian cell cycle models. The species as they occur in the Integrated cell cycle network are listed below, along with the specie names as they occur in the original manuscripts where the Csikasz2, Novak, Conradie models were described. The mammalian cell cycle models could all be constructed with 25 of the 54 variable species from the integrated cell cycle network. Species that occured in all models (highlighted in bold) were used to compare the respective models.

	Mammalian cell Models		
Specie	**Csikasz2**	**Novak**	**Conradie**
C5 (CLB5/SIC1)	**CycA - actCycA**	**cycA:Kip1**	**cycA:Kip1**
CDC14	Cdc20A	-	-
CDC20A	**Cdc20A**	**Cdc20**	**Cdc20**
CDC20I	**Cdc20T - Cdc20A**	**Cdc20T - Cdc20**	**Cdc20T - Cdc20**
CDH1A	**Cdh1**	**Cdh1**	**Cdh1**
CLB2 (clb2/cdk)	**actCycB**	**cycB**	**cycB**
CLB2p	CycB - actCycB - TriB	-	-
CLB5	**actCycA**	**cycA**	**cycA**
CLN2	**actCycE**	**cycE**	**cycE**
CLN2/SIC1	**CycE - actCycE**	**cycE:Kip1**	**cycE:Kip1**
CYCD	-	cycD	cycD
CYCD/SIC1	-	cycD:Kip1	cycD:Kip1
DRG	-	DRG	DRG
E2F	-	E2F	E2F
E2Fp	-	-	E2Fp

Continued on Next Page...

Specie	**Csikasz2**	**Novak**	**Conradie**
ERG	-	ERG	ERG
GM	-	GM	GM
IEP	**APCP**	**IEP**	**IEP**
MASS	**mass**	**mass**	**mass**
PPX	-	PPX	PPX
Rb	-	-	Rb
Rb/E2F	-	-	Rb/E2F
Rb/pE2F	-	-	Rb/pE2F
Rbp	-	-	Rbp
SIC1	**CKI - CycA - CycE + actCycE + actCycA**	**Kip1**	**Kip1**

Table 5.4: Species occuring in the general cell cycle models. The species as they occur in the Integrated cell cycle network are listed below, along with the specie names as they occur in the original manuscripts where the Srividhya, Surovstev and Tyson2 models were described. The general cell cycle models could all be constructed with 11 of the 54 variable species from the integrated cell cycle network. Species that occured in all models (highlighted in bold) were used to compare the respective models.

	General cell cycle models		
Specie	**Srividhya**	**Surovstev**	**Tyson2**
CDC20A	-	Cdc20a	Cdc20A
CDC20I	-	Cdc20	Cdc20T - Cdc20A
CDH1A	**APC-P**	**Cdh1a**	**Cdh1**
CDH1I	-	Cdh1	-
cdk	free Cdk	-	-
clb2	cyclin	-	-
CLB2 (clb2/cdk)	**MPF**	**Clnb:Cdk**	**CycB**
IEP	-	-	IE
MASS	**M**	**Vcyt**	**M**
MIH1	Cdc25P	-	-
SWE1	Wee1	-	-

Chapter 6

General discussion

In this thesis we addressed the following central research question: "Is it possible to quantify the control exerted by the processes in the cell cycle network on the checkpoints of G1/S transition?" For this we analyzed, within the framework of MCA, several kinetic models for the cell cycle of mammalian and budding yeast cells. We first developed an extension to the existing MCA framework to quantify the control of dynamic systems (see Chapter 3). With this tool we analyzed the control distribution for the positioning of the restriction point (RP, a checkpoint in the G1 phase) in a mammalian cell cycle model. The results as presented in Chapter 4, showed that several processes controlled the positioning of RP, most notably those involved in: 1) the interaction between Rb and E2F transcription factor; 2) the synthesis of DRG and Cyclin D/Cdk4 in response to growth signals; 3) the E2F dependent Cyclin E/Cdk2 synthesis reaction; and 4) p27 formation reaction. In Chapter 4 we also show that these processes likely affect the restriction point via the Cyclin E/Cdk2:p27 complex.

We used an operational definition for the restriction point, with which we could analyze the control distribution for this checkpoint. With respect to a mass assessment checkpoint no such definition could be used; actually the existence of a mass-assesment point in mammalian cells is a point of debate. To check whether a mass-assessment point exists, we analyzed in a comparative study between mammalian and budding yeast cell cycle models, the robustness of cell

size at the G1/S transition point (see Chapter 5). For this we first had to analyze the control of the G1/S transition point. Strikingly, in all the detailed models that were analyzed two reaction blocks had by far the strongest control on the G1/S transition point, the first being the mass accumulation block and the second the Clb2 synthesis and degradation block. In contrast to the similarity for the control distribution on the G1/S transition point, no good agreement between the mammalian cell cycle models and the yeast models was observed for the robustness of cell size at the G1/S transition point. Our analysis showed that in yeast a mass "correction" mechanism exists in the G1 phase that makes the cell size at the G1/S transition point very robust to perturbations in the network reactions. For mammalian cell cycle models we observed that the cell mass at the G1/S transition point was not as robustly regulated as in the yeast models, and we could not find indications of a "correction" mechanism; cell size at the beginning of the G1 phase was equally robust for reaction perturbations as cell size at the G1/S transition point.

Three core models did not display similar G1/S transition control distributions as were observed in the more detailed models. By adding a starter kinase (Cln2) and a cyclin dependent kinase inhibitor (Sic1) to one of these core models, we showed in Chapter 5, that these two reactions changed the core model such that it displayed the same control distribution on G1/S positioning (after Cln2 addition) as was observed in the detailed models and made the model robust for cell size at the G1/S transition point (after both Cln2 and Sic1 were added to the model). Here it should be noted that it is not just the presence of Cln2 and Sic1 that leads to the changes in the core model, but more importantly the way these components interact with the other components. Cln2 and Sic1 are present in both the mammalian and yeast models, but only in yeast does this lead to cell-size stabilization at the G1/S transition point. This could be due to the different roles the proteins play in these organisms, in yeast Sic1 stabilizes Clb2 but not Cln2 while in mammalian cells this is exactly reversed (i.e. Sic1 stabilizes Cln2 but not Clb2).

In this thesis we have used a Systems Biology approach to address a number of key questions on control of the G1/S transition. Important for such an

approach is the iterative cycle between theory, modeling and experiment. We have here focused on the first two tiers of this cycle: theory development and modeling analysis. We extended the MCA framework to include control analysis of dynamic systems, specifically the analysis of time dependent behavior (e.g. species concentrations at a specific time point). This was an important extension of the framework, which could only deal with time invariant behavior (e.g. frequency of oscillation in the limit cycle). We have also developed generic tools for model analysis: 1) we analyzed in detail how the control of systems behavior by processes can be related to specific species in the system (i.e. control of the restriction point via the CyclinE/Cdk2 complex) and 2) we made a comparative analysis between a set of models, using a modular approach. The first method is important to merge the MCA approach (analyzing systems in terms of processes) and the traditional approach for dynamic systems analysis (in terms of model species). The comparative analysis tool is important in view of the large number of models that are being generated and stored in databases but not compared. We have illustrated how model comparisons can be made, even for models that differ largely in the detail with which the processes are being modeled. We addressed specific problems in these comparisons: such as testing whether a consensus view exists in the models on control distribution of the G1/S transition point, or whether a mass assessment checkpoint exists in mammalian cell cycle models.

We needed to select a subset of models to make the comparative analysis useful. For instance the existence of certain species in the model if these are essential for testing a hypothesis (e.g. mass is essential to test for robustness of mass), or for defining a state in the system (e.g. Cdh1 decline marks the G1/S transition point). Such a selection clearly limits the number of models that can be included in the analysis (and thereby its generality), but it strengthens the analysis because more specific questions can be addressed. Although the requirements for our model selection does not seem overly stringent, they did limit us to a subset of models mainly produced by two research groups (the Tyson group at Virginia Tech, USA and the Novak group, now at Oxford, UK). The main reason for the restricted number of models was the requirement that

the models should describe a complete cell cycle. Most of the models on the cell cycle focus on a subset of the cell cycle. It would be an enormous improvement if modeling efforts by groups could be combined, even if it were only by formulating a very basic framework for the cell cycle. Such efforts would necessitate standardization e.g. of units for rates and concentrations and an agreement must be made for variable names, but these seem minimal efforts compared to the hugh gain that could be made in a combined effort to modeling the cell cycle.

We have not extensively used the third tier of the iterative cycle: experimentation. Of course experimentation was involved in construction of most of the models that we have analyzed, and MCA makes a direct connection to experimentation via its formulation in terms of perturbations of reaction steps, but we have not focused on experimentation ourselves. Irrespective of this, we should still discuss the relevance of our work for experimental cell cycle studies. One of the most common approaches in experimental analysis of the cell cycle is the use of knock-out mutants to study the role of a molecular specie. We should stress that this approach is essentially different from the MCA approach towards perturbations. Whereas in MCA infinitesimally small changes are made to study the system at its physiological state, in a knock-out perturbation a component is completely removed from the system thereby making a big change, which could easily have moved the system far away from its physiological state. This could lead to very different results, for instance in our MCA analysis on control of mass at the transition point we observed that the three modules around active Cdc20, Cln2 and CDh1 had the highest control. However, from knock-out studies on these three components completely different results were obtained, and none of these pointed at the role of the component in controlling mass[5,23,70]. More subtle than deletion mutants would be the use of inhibitor titrations to study the role of processes on systems behavior. Anti-cancer therapeutics, such as synthetic cyclin-dependent kinase inhibitors have been used in cell cycle studies[13]. Such inhibitor studies have as major advantages above deletion mutants that the system can be studied at its physiological state and effects of small perturbations can be inferred from extrapolation to a zero concentration of the inhibitor.

It has been argued that systems level modeling of the cell cycle requires the

integration of 'omics' data, such as proteomic data, with an appropriate mathematical framework such as dynamic modeling[46]. To integrate such large data-sets good mathematical analysis tools are essential, and these top-down and hybrid type of approaches are important to model whole cell behavior, for which detailed molecular information is not available. In this thesis we have focused on models that describe the cell cycle at a much lower level of detail, for the analysis of which we used the mathematical framework of MCA. Whereas these models do not describe enormous data-sets, they have been very useful for testing hypotheses on regulation and control of the G1/S transition state. We have stressed in this thesis the role of model analysis and model comparison. These aspects highlight additional roles for mathematical models, and we have demonstrated how by using such analysis tools long standing debates can be addressed. For instance, we tested whether we could find indications for a cell size controller in the G1 phase of the cell cycle models. This is an open question, and still very much under debate as indicated in the July 2009 issue of *Science*[25,77] By casting the question in the MCA framework, we could find a consensus answer in our comparative approach: in yeast there appears to be such a mass assessment point in the G1 phase while we could not find such a checkpoint in the mammalian models.

Bibliography

1. L. Acerenza. Control of metabolic processes. *Plenum Press, New York (Cornish-Bowden, A., Cárdenas, M.L. (Eds.))*, Chapter 25:297–302, 1990.

2. L. Acerenza and H. Kacser. Enzyme kinetics and metabolic control. a method to test and quantify the effect of enzymic properties on metabolic variables. *Biochem. Journal*, 269:697–707, 1990.

3. L. Acerenza, H. M. Sauro, and H. Kacser. Control analysis of time-dependent metabolic systems. *Journal of Theoretical Biology*, 137(4):423–444, 1989.

4. B. D. Aguda and Y. Tang. The kinetic origins of the restriction point in the mammalian cell cycle. *Cell Proliferation*, 32(5):321–335, 1999.

5. G. Alexandru, W. Zachariae, A. Schleiffer, and K. Nasmyth. Sister chromatid separation and chromosome re-duplication are regulated by different mechanisms in response to spindle damage. *The EMBO Journal*, 18(10):2707–2721, 1999.

6. M. Barberis and E. Klipp. Insights into the network controlling the G1/S transition in budding yeast. *Genome Informatics. International Conference on Genome Informatics*, 18:85–99, 2007.

7. M. Barberis, E. Klipp, M. Vanoni, and L. Alberghina. Cell size at s phase initiation: an emergent property of the G1/S network. *PLoS Computational Biology*, 3(4):e64, 2007.

8. M. Bier, B. Teusink, B. N. Kholodenko, and H. V. Westerhoff. Control analysis of glycolytic oscillations. *Biophysical Chemistry*, 62(1-3):15–24, 1996.

9. M. V. Blagosklonny and A. B. Pardee. The restriction point of the cell cycle. *Cell cycle (Georgetown, Tex.)*, 1:103–10, 2002.

10. F. J. Bruggeman and H. V. Westerhoff. The nature of systems biology. *Trends in Microbiology*, 15(1):45–50, 2007.

11. F. J. Bruggeman, H. V. Westerhoff, and F. C. Boogerd. BioComplexity: a pluralist research strategy is necessary for a mechanistic explanation of the "live" state. *Philosophical Psychology*, 15(4):411–440, 2002.

12. F. J. Bruggeman, H. V. Westerhoff, J. B. Hoek, and B. N. Kholodenko. Modular response analysis of cellular regulatory networks. *Journal of Theoretical Biology*, 218:507–520, 2002.

13. C. Chassagnole, R. C. Jackson, N. Hussain, L. Bashir, C. Derow, J. Savin, and D. A. Fell. Using a mammalian cell cycle simulation to interpret differential kinase inhibition in anti-tumour pharmaceutical development. *Bio Systems*, 83(2-3):91–97, 2006.

14. K. C. Chen, L. Calzone, A. Csikasz-Nagy, F. R. Cross, B. Novak, and J. J. Tyson. Integrative analysis of cell cycle control in budding yeast. *Molecular Biology of the Cell*, 15(8):3841–3862, 2004.

15. K. C. Chen, A. Csikasz-Nagy, B. Gyorffy, J. Val, B. Novak, and J. J. Tyson. Kinetic analysis of a molecular model of the budding yeast cell cycle. *Molecular Biology of the Cell*, 11(1):369–391, 2000.

16. I. M. Chu, L. Hengst, and J. M. Slingerland. The cdk inhibitor p27 in human cancer: prognostic potential and relevance to anticancer therapy. *Nat Rev Cancer*, 8(4):253–67, 2008.

17. I. Conlon and M. Raff. Differences in the way a mammalian cell and yeast cells coordinate cell growth and cell-cycle progression. *Journal of Biology*, 2(1):7, 2003.

18. R. Conradie, F. J. Bruggeman, A. Ciliberto, A. Csikasz-Nagy, B. Novak, H. V. Westerhoff, and J. L. Snoep. Restriction point control of the mammalian cell cycle via the cyclin e/cdk2:p27 complex. *FEBS Journal*, submitted, 2009.

19. R. Conradie, H. V Westerhoff, J. -H.S Hofmeyr, J. M Rohwer, and J. L Snoep. Summation theorems for flux and concentration control coefficients of dynamic systems. *Systems Biology, IEE Proceedings*, 153(5):314–317, 2006.

20. S. Cooper. Control and maintenance of mammalian cell size. *BMC Cell Biology*, 5(1):35, 2004.

21. A. Csikász-Nagy, D. Battogtokh, K. C. Chen, B. Novák, and J. J. Tyson. Analysis of a generic model of eukaryotic cell-cycle regulation. *Biophysical Journal*, 90(12):4361–4379, 2006.

22. O. V. Demin, H. V. Westerhoff, and B. N. Kholodenko. Control analysis of stationary forced oscillations. *Journal of Physical Chemistry B*, 103(48):10695–10710, 1999.

23. L. Dirick, T. Böhm, and K. Nasmyth. Roles and regulation of Cln-Cdc28 kinases at the start of the cell cycle of saccharomyces cerevisiae. *The EMBO Journal*, 14(19):4803–4813, 1995.

24. F. B. du Preez, R. Conradie, G. P. Penkler, K. Holm, F. L. J. van Dooren, and J. L. Snoep. A comparative analysis of kinetic models of erythrocyte glycolysis. *Journal of Theoretical Biology*, 252(3):488–496, 2008.

25. B. A. Edgar and K. J. Kim. Sizing up the cell. *Science*, 325(5937):158–159, 2009.

26. M. Erlanson, C. Portin, B. Linderholm, J. Lindh, G. Roos, and G. Landberg. Expression of cyclin e and the cyclin-dependent kinase inhibitor p27 in malignant lymphomas-prognostic implications. *Blood*, 92:770–7, 1998.

27. J. E. Ferrell. Tripping the switch fantastic: how a protein kinase cascade can convert graded inputs into switch-like outputs. *Trends in Biochemical Sciences*, 21(12):460–466, 1996.

28. C. Geisen, H. Karsunky, R. Yucel, and T. Moroy. Loss of p27Kip1 cooperates with cyclin e in t-cell lymphomagenesis. *Oncogene*, 22:1724–1729, 2003.

29. A. Gilman and A. P. Arkin. Genetic "code": representations and dynamical models of genetic components and networks. *Annu. Rev. Genomics Hum. Genet.*, 3:341–369, 2002.

30. A. Goldbeter and S. R. Caplan. Oscillatory enzymes. *Annual Review of Biophysics and Bioengineering*, 5:449–476, 1976.

31. A. Goldbeter and D. E. Koshland. An amplified sensitivity arising from covalent modification in biological systems. *Proceedings of the National Academy of Sciences of the United States of America*, 78(11):6840–6844, 1981.

32. A. Goldbeter and R. Lefever. Dissipative structures for an allosteric model. application to glycolytic oscillations. *Biophysical Journal*, 12(10):1302–1315, 1972.

33. T. Haberichter, B. Mädge, R. A. Christopher, N. Yoshioka, A. Dhiman, R. Miller, R. Gendelman, S. V. Aksenov, I. G. Khalil, and S. F. Dowdy. A systems biology dynamical model of mammalian g1 cell cycle progression. *Mol Syst Biol*, 3:84, 2007.

34. L. H. Hartwell, J. J. Hopfield, S. Leibler, and A. W. Murray. From molecular to modular cell biology. *Nature*, 402:C47–C52, 1999.

35. L. H. Hartwell and M. W. Unger. Unequal division in saccharomyces cerevisiae and its implications for the control of cell division. *J. Cell Biol.*, 75(2):422–435, 1977.

36. V. Hatzimanikatis, K. H. Lee, and J. E. Bailey. A mathematical description of regulation of the G1-S transition of the mammalian cell cycle. *Biotechnology and Bioengineering*, 65(6):631–637, 1999.

37. H. Hayashi, N. Ogawa, N. Ishiwa, T. Yazawa, Y. Inayama, T. Ito, and H. Kitamura. High cyclin e and low p27/Kip1 expressions are potentially poor prognostic factors in lung adenocarcinoma patients. *Lung Cancer (Amsterdam, Netherlands)*, 34(1):59–65, 2001.

38. R. Heinrich and T. A. Rapoport. A linear Steady-State treatment of enzymatic chains. *European Journal of Biochemistry*, 42(1):97–105, 1974.

39. R. Heinrich and T. A. Rapoport. A linear steady-state treatment of enzymatic chains. general properties, control and effector strength. *European Journal of Biochemistry / FEBS*, 42(1):89–95, 1974.

40. R. Heinrich and T. A. Rapoport. Mathematical analysis of multienzyme systems. II. steady state and transient control. *Bio Systems*, 7(1):130–136, 1975.

41. R. Heinrich and C. Reder. Metabolic control analysis of relaxation processes. *Journal of Theoretical Biology*, 151(3):343–350, 1991.

42. J. H. Hofmeyr and A. Cornish-Bowden. Co-response analysis: a new experimental strategy for metabolic control analysis. *Journal of Theoretical Biology*, 182(3):371–80, 1996.

43. J. H. Hofmeyr and H. V. Westerhoff. Building the cellular puzzle: control in multi-level reaction networks. *Journal of Theoretical Biology*, 208(3):261–285, 2001.

44. J. J. Hornberg, F. J. Bruggeman, B. Binder, C. R. Geest, A. J. M. Bij de Vaate, J. Lankelma, R. Heinrich, and H. V. Westerhoff. Principles behind the multifarious control of signal transduction. *FEBS Journal*, 272(1):244–258, 2005.

45. B. P. Ingalls. Autonomously oscillating biochemical systems: parametric sensitivity of extrema and period. *Systems Biology*, 1(1):62–70, 2004.

46. B. P. Ingalls, B. P. Duncker, D. R. Kim, and B. J. McConkey. Systems level modeling of the cell cycle using budding yeast. *Cancer Informatics*, 3:357–370, 2007.

47. B. P. Ingalls and H. M. Sauro. Sensitivity analysis of stoichiometric networks: an extension of metabolic control analysis to non-steady state trajectories. *Journal of Theoretical Biology*, 222(1):23–36, 2003.

48. H. Kacser and J. A. Burns. The control of flux. *Symposia of the Society for Experimental Biology*, 27:65–104, 1973.

49. B. N. Kholodenko, O. V. Demin, and H. V. westerhoff. Control analysis of periodic phenomena in biological systems. *Journal of Physical Chemistry B*, 101(11):2070–2081, 1997.

50. D. Killander and A. Zetterberg. A quantitative cytochemical investigation of the relationship between cell mass and initiation of DNA synthesis in mouse fibroblasts in vitro. *Experimental Cell Research*, 40(1):12–20, 1965.

51. K. W. Kohn. Molecular interaction map of the mammalian cell cycle control and DNA repair systems. *Molecular Biology of the Cell*, 10(8):2703–2734, 1999.

52. S. Kumar and J. C. Feidler. BioSPICE: a computational infrastructure for integrative biology. *OMICS*, 7:225, 2003.

53. E. S. Lander and R. A. Weinberg. Genomics: journey to the center of biology. *Science*, 287:1777–1782, 2000.

54. J. Maddox. Cell-cycle regulation by numbers. *Nature*, 369:437, 1994.

55. S. Moreno and P. Nurse. Regulation of progression through the g1 phase of the cell cycle by the rum1+ gene. *Nature*, 367(6460):236–242, 1994.

56. B. Novák and J. J. Tyson. A model for restriction point control of the mammalian cell cycle. *Journal of Theoretical Biology*, 230(4):563–579, 2004.

57. P. Nurse. The incredible life and times of biological cells. *Science*, 289:1711–1716, 2000.

58. A. B. Pardee. A restriction point for control of normal animal cell proliferation. *Proceedings of the National Academy of Sciences of the United States of America*, 71:1286–90, 1974.

59. J. J. Del Pizzo, A. Borkowski, S. C. Jacobs, and N. Kyprianou. Loss of cell cycle regulators p27Kip1 and cyclin e in transitional cell carcinoma of the bladder correlates with tumor grade and patient survival. *Am J Pathol*, 155:1129–1136, 1999.

60. M. D. Planas-Silva and R. A. Weinberg. The restriction point and control of cell proliferation. *Current opinion in cell biology*, 9:768–72, 1997.

61. K. A. Reijenga, J. L. Snoep, J. A. Diderich, H. W. van Verseveld, H. V. Westerhoff, and B. Teusink. Control of glycolytic dynamics by hexose transport in saccharomyces cerevisiae. *Biophysical Journal*, 80(2):626–634, 2001.

62. K. A. Reijenga, Y. M. G. A. van Megen, B. W. Kooi, B. M. Bakker, J. L. Snoep, H. W. van Verseveld, and H. V. Westerhoff. Yeast glycolytic oscillations that are not controlled by a single oscillophore: a new definition of oscillophore strength. *Journal of Theoretical Biology*, 232(3):385–398, 2005.

63. K. A. Reijenga, H. V. Westerhoff, B. N. Kholodenko, and J. L. Snoep. Control analysis for autonomously oscillating biochemical networks. *Biophysical Journal*, 82(1 Pt 1):99–108, 2002.

64. I. Rupes. Checking cell size in yeast. *Trends in Genetics: TIG*, 18(9):479–485, 2002.

65. P. Schraml, C. Bucher, H. Bissig, A. Nocito, P. Haas, K. Wilber, S. Seelig, J. Kononen, M. J. Mihatsch, S. Dirnhofer, and G. Sauter. Cyclin e overexpression and amplification in human tumours. *The Journal of Pathology*, 200(3):375–82, 2003.

66. D. A. Skalicky, J. G. Kench, D. S., M. J. Coleman, R. L. Sutherland, S. M. Henshall, E. A. Musgrove, and A. V. Biankin. Cyclin e expression and outcome in pancreatic ductal adenocarcinoma. *Cancer Epidemiology, Biomark-*

ers & Prevention: A Publication of the American Association for Cancer Research, Cosponsored by the American Society of Preventive Oncology, 15(10):1941–7, 2006.

67. J. L. Snoep. The silicon cell initiative: working towards a detailed kinetic description at the cellular level. *Current Opinion in Biotechnology*, 16(3):336–343, 2005.

68. J. L. Snoep and H. V. Westerhoff. *"From isolation to integration, a systems biology approach for building the Silicon Cell". Systems Biology: Definitions and Perspectives: p7*. Springer-Verlag, 2005.

69. J. Srividhya and M. S. Gopinathan. A simple time delay model for eukaryotic cell cycle. *Journal of Theoretical Biology*, 241(3):617–627, 2006.

70. D. Stuart and C. Wittenberg. CLN3, not positive feedback, determines the timing of CLN2 transcription in cycling cells. *Genes & Development*, 9(22):2780–2794, 1995.

71. I. V. Surovstev, J. J. Morgan, and P. A. Lindahl. Whole-cell modeling framework in which biochemical dynamics impact aspects of cellular geometry. *Journal of Theoretical Biology*, 244(1):154–166, 2007.

72. A. Sveiczer, B. Novak, and J. M. Mitchison. Size control in growing yeast and mammalian cells. *Theoretical Biology and Medical Modelling*, 1(1):12, 2004.

73. T. Tamiya, S. Mizumatsu, Y. Ono, T. Abe, K. Matsumoto, T. Furuta, and T. Ohmoto. High cyclin e/low p27Kip1 expression is associated with poor prognosis in astrocytomas. *Acta Neuropathologica*, 101(4):334–40, 2001.

74. Y. Tashima, H. Hamada, M. Okamoto, and T. Hanai. Prediction of key factor controlling G1/S phase in the mammalian cell cycle using system analysis. *Journal of Bioscience and Bioengineering*, 106(4):368–374, 2008.

75. J. J. Tyson, A. Csikasz-Nagy, and B. Novak. The dynamics of cell cycle regulation. *BioEssays: News and Reviews in Molecular, Cellular and Developmental Biology*, 24(12):1095–1109, 2002.

76. J. J. Tyson and B. Novak. Regulation of the eukaryotic cell cycle: molecular antagonism, hysteresis, and irreversible transitions. *Journal of Theoretical Biology*, 210(2):249–263, 2001.

77. A. Tzur, R. Kafri, V. S. LeBleu, G. Lahav, and M. W. Kirschner. Cell growth and size homeostasis in proliferating animal cells. *Science (New York, N.Y.)*, 325(5937):167–171, 2009.

78. C. van Gend, R. Conradie, F. B. du Preez, and J. L. Snoep. Data and model integration using JWS online. *In Silico Biology*, 7(2 Suppl):S27–35, 2007.

79. W. A. Wells. Does size matter? *J. Cell Biol.*, 158(7):1156–1159, 2002.

80. H. V. Westerhoff, M. A. Aon, K. van Dam, S. Cortassa, D. Kahn, and M. van Workum. Dynamical and hierarchical coupling. *Biochimica Et Biophysica Acta*, 1018:142–146, 1990.

81. H. V. Westerhoff and D. Kahn. Control involving metabolism and gene expression. *Acta Biotheoretica*, 41(1):75–83, 1993.

82. H. V. Westerhoff, A. Kolodkin, R. Conradie, S. J. Wilkinson, F. J. Bruggeman, K. Krab, J. H. van Schuppen, H. Hardin, B. M. Bakker, M. J. Moné, K. N. Rybakova, M. Eijken, H. J. P. van Leeuwen, and J. L. Snoep. Systems biology towards life in silico: mathematics of the control of living cells. *Journal of Mathematical Biology*, 58(1-2):7–34, 2009.

83. J. Yaglom, M. H. Linskens, S. Sadis, D. M. Rubin, B. Futcher, and D. Finley. p34Cdc28-mediated control of cln3 cyclin degradation. *Molecular and Cellular Biology*, 15(2):731–741, 1995.

84. G. Yao, T. J. Lee, S. Mori, J. R Nevins, and L. You. A bistable Rb-E2F switch underlies the restriction point. *Nature Cell Biology*, 10(4):476–482, 2008.

85. A. Zetterberg and O. Larsson. Kinetic analysis of regulatory events in g1 leading to proliferation or quiescence of swiss 3T3 cells. *Proceedings of the National Academy of Sciences*, 82:5365–5369, 1985.

86. Q. Zhou, Q. He, and L.-J. Liang. Expression of p27, cyclin e and cyclin a in hepatocellular carcinoma and its clinical significance. *World journal of gastroenterology : WJG*, 9:2450–4, 2003.